

University of Louisville

ThinkIR: The University of Louisville's Institutional Repository

Electronic Theses and Dissertations

8-2023

Design and evaluation of a multi-functional surgical device for microgravity surgeries.

Sienna Shacklette
University of Louisville

Follow this and additional works at: <https://ir.library.louisville.edu/etd>



Part of the [Biomedical Engineering and Bioengineering Commons](#)

Recommended Citation

Shacklette, Sienna, "Design and evaluation of a multi-functional surgical device for microgravity surgeries." (2023). *Electronic Theses and Dissertations*. Paper 4181.
<https://doi.org/10.18297/etd/4181>

This Master's Thesis is brought to you for free and open access by ThinkIR: The University of Louisville's Institutional Repository. It has been accepted for inclusion in Electronic Theses and Dissertations by an authorized administrator of ThinkIR: The University of Louisville's Institutional Repository. This title appears here courtesy of the author, who has retained all other copyrights. For more information, please contact thinkir@louisville.edu.

Design And Evaluation of a Multi-Functional Surgical Device
For Microgravity Surgeries

by

Sienna Shacklette

B.S. Bioengineering 2021

University of Louisville

Submitted to the Faculty of the Department of Bioengineering

in partial fulfillment of

BE 697 – Master of Engineering

August 9th, 2023

Design And Evaluation of a Multi-Functional Surgical Device
For Microgravity Surgeries

Submitted by:

Sienna Shacklette

A Thesis Approved on: 8/9/2023

By the following Reading and Examination Committee:

Thomas J. Roussel, Jr. Digitally signed by Thomas J. Roussel, Jr.
Date: 2023.08.01 12:50:03 -04'00'

Thomas J. Roussel, Jr. Ph.D.
Thesis Chair

George M Pantalos Digitally signed by George M Pantalos
Date: 2023.08.01 16:00:02 -04'00'

George Pantalos, Ph.D.
Thesis Co-Chair

Digitally signed by Christopher M. Richards
Date: 2023.08.01 20:11:25 -04'00'

Christopher Richards, Ph.D.
Thesis Committee Member

ACKNOWLEDGEMENTS

I would like to thank my mentors for working with me through the ups, downs, and late nights through these projects. I'd like to thank Dr. Pantalos for taking me under his wing as a sophomore in college and taking the chance on me as a young kid with no skills. I'd also like to thank Dr. Roussel for working with me during all hours and helping me through the pre-flight campaign emergencies. I'd like to thank them all for supporting me through my first big project and providing me with any help I asked for in order to complete this project.

ABSTRACT

With the increase in commercial space flight operations and the possibility of heading further than we have ever been before on the horizon, this creates a host of challenges that have to be overcome. This includes the need for medical and surgical capabilities in space. Currently in the case of medical accidents, astronauts are sent back down to earth usually within twenty-four hours, after being made stable. In addition, there is very little communication delay between the ISS and the ground, only being a few seconds. However, when it comes to missions further beyond the ISS, the communication time delay, the amount of time needed to get back to earth and the overall danger of the mission increases. This increases the need for the astronaut team to be able to provide their own independent health and surgical care. For this, new techniques and devices need to be developed to fill this gap in current capabilities. With this new avenue opened, there are a few additional criteria that need to be kept in mind during the development: 1) space and weight on spacecraft is very valuable and everything needs to be as compact as possible, and must serve multiple purposes, 2) all technology must be user friendly due to the already stressful situation of spaceflight, additionally, the person performing the surgical tasks will likely be a doctor but may not be a surgeon, and 3) there will be a large communication delay so telemedicine is not a viable option. With all of this in mind, the Multi-

Functional Surgical Device (MFSD) was envisioned. This device would be able to complete the five commonly used surgical functions: suction, irrigation, illumination, visualization, and cautery, all wrapped up in one device. This would fulfill the task of creating specialty surgical equipment with space travel in mind. This device and its attached system could be stored with an ISS stowage locker, and easily set up within minutes when needed. The design was created to be as comfortable and intuitive as possible for use. Over the years, the MFSD went through six different designs until the most recent design incorporated all five of the functions, including a dual-temperature cautery. This final design was proven to work under zero gravity conditions in a series of parabolic flights. While this current design still needs to be improved, it is a proof-of-concept that multi-functional surgical devices can be created and used for space medicine applications.

TABLE OF CONTENTS

| | |
|--|------|
| ACKNOWLEDGEMENTS..... | iv |
| ABSTRACT | v |
| TABLE OF CONTENTS..... | vii |
| LIST OF FIGURES | x |
| LIST OF TABLES..... | xiii |
| I. INTRODUCTION..... | 1 |
| 1.1 Microgravity Standard Practices..... | 1 |
| 1.2 Problem Statement: Multi-Functional Surgical Device..... | 2 |
| 1.3 Project Specific Aims..... | 3 |
| II. BACKGROUND..... | 5 |
| 2.1. Problem Statement..... | 8 |
| 2.2. Existing Multi-Functional Medical Devices..... | 8 |
| 2.3. Cautery..... | 10 |
| 2.2.1 Electrosurgery..... | 11 |
| 2.2.2 Thermal Cautery | 11 |
| 2.4. Multifunctional Surgical Devices: Implications | 12 |
| 2.5. Previous Developments..... | 12 |
| 2.5.1 Aqueous Immersion Surgical System | 12 |
| 2.5.2 Surgical Immersion Dome..... | 14 |
| 2.5.3 Leak-Free Trocars..... | 16 |
| 2.5.4 Fluid Management System | 17 |
| 2.5.5 The Experiment Glovebox | 18 |
| 2.5.6 Modular Experiment Board | 19 |
| 2.6. Previous MFSD Developments | 20 |
| 2.6.1 Fall 2016 Capstone..... | 20 |
| 2.6.2 Summer 2018 MEng Thesis..... | 22 |
| 2.6.3 Fall 2020 Capstone (Cautery Prototype)..... | 27 |

| | |
|---|----|
| III. MATERIALS AND METHODS | 30 |
| 3.1. Design Criteria..... | 30 |
| 3.1.1 Objectives | 30 |
| 3.1.2 Technical Specifications..... | 31 |
| 3.2. Device Hardware..... | 32 |
| 3.2.1 Fluid Components..... | 32 |
| 3.2.2 Peristaltic Pumps | 33 |
| 3.2.3 Button Switch Configuration..... | 34 |
| 3.2.4 Button Switch Circuit Schematic | 34 |
| 3.2.5 Pushbutton Switch Caps..... | 35 |
| 3.2.6 Control Printed Circuit Board | 36 |
| 3.2.7 Combined LED Light and Camera | 38 |
| 3.2.8 Suction and Irrigation Wand..... | 39 |
| 3.2.9 Cautery Element | 41 |
| 3.2.10 Clamshell Handle | 45 |
| 3.3. Design V..... | 45 |
| 3.4. Design VI..... | 47 |
| 3.5. Tablet Controller for Flight Testing | 50 |
| 3.6. Portable Bronchoscope Monitor | 51 |
| 3.7. Microcontroller..... | 52 |
| 3.8. Flight Hardware | 52 |
| 3.9. Control Software..... | 55 |
| 3.10. Verification and Validation | 55 |
| 3.10.1. Leak Testing | 55 |
| 3.10.2. Suction and Irrigation Testing | 56 |
| 3.10.3. Illumination and Visualization Testing | 56 |
| 3.10.4. Cautery Testing..... | 57 |
| 3.10.5. Stand-Alone Control Testing..... | 58 |
| 3.11. Flight Testing..... | 60 |
| IV. RESULTS | 62 |
| 4.1. Illumination and Visualization Integration | 62 |
| 4.2. Suction and Irrigation Wand | 66 |
| 4.3. Cautery Element..... | 66 |

| | | |
|-------|--|----|
| 4.4. | Clamshell Handle | 69 |
| 4.5. | Control Printed Circuit Board | 70 |
| 4.6. | Software | 71 |
| 4.7. | Benchtop Testing | 71 |
| 4.7.1 | Leak Testing..... | 71 |
| 4.7.2 | Suction and Irrigation Testing..... | 71 |
| 4.7.3 | Illumination and Visualization Testing | 72 |
| 4.7.4 | Cautery Testing..... | 74 |
| 4.7.5 | Stand-Alone Control Testing | 75 |
| 4.8. | In Flight Testing | 76 |
| V. | DISCUSSION | 80 |
| 5.1. | Design Review | 80 |
| 5.1.1 | MFSD Shaft | 80 |
| 5.1.2 | MFSD Handle | 80 |
| 5.1.3 | Functionality..... | 81 |
| 5.1.4 | Software and Electronics | 81 |
| 5.2. | Overall Summary..... | 82 |
| 5.3. | Limitations | 82 |
| 5.4. | Future Work..... | 83 |
| 5.4.1 | Wand Handle | 83 |
| 5.4.2 | Cautery Temperature Adjustment..... | 83 |
| 5.4.3 | Cautery Element | 84 |
| VI. | CONCLUSION..... | 85 |
| | REFERENCES | 86 |
| VII. | Appendix A: Arduino Test Code | 89 |
| VIII. | Appendix A: LabVIEW Test Code | 98 |

LIST OF FIGURES

| | |
|---|----|
| Figure 1: The ENDOPATH Electrosurgery PROBE PLUS II | 9 |
| Figure 2: Bovie Suction Coagulator | 9 |
| Figure 3: Medtronic Aquamantys MPR Bipolar Sealers..... | 10 |
| Figure 4: Side view of the University of Louisville suborbital AISS experiment, showing the Design IV MFSD that was implemented for suborbital flight..... | 13 |
| Figure 5: Overhead view of the University of Louisville and the Carnegie Mellon/Cornell University suborbital AISS systems in the Suborbital Glovebox during suborbital flight | 14 |
| Figure 6: Surgical Immersion Dome with 3mm and 8mm Leak-Free Trocar inserted..... | 15 |
| Figure 7: Eight surgical immersion domes with the attached loban and Duoderm seal laminate, filling and emptying ports, and the surgical instrument ports incorporated into the dome..... | 16 |
| Figure 8: Isometric rendering of a 5mm Leak-Free Trocar..... | 17 |
| Figure 9: Experiment glovebox with two arm access ports open..... | 18 |
| Figure 10: MFSD Design I prototype | 20 |
| Figure 11: The fluid circuit for Design I of the MFSD | 21 |
| Figure 12: A rendering of Design II of the MFSD..... | 22 |
| Figure 13: A rendering of Design III of the MFSD | 23 |
| Figure 14: A rendering of Design IV of the MFSD..... | 24 |
| Figure 15: An exploded view rendering of Design IV of the MFSD..... | 25 |
| Figure 16: 3D model of shaft Design IV of the MFSD (Length = 10.5in)..... | 26 |
| Figure 17: 3D model showing tip of the shaft for the Design IV of the MFSD..... | 26 |
| Figure 18: Heating element, showing the copper, fiberglass tubing, and the coiled nichrome wire | 28 |
| Figure 19: Full image of the original cautery prototype test setup | 29 |
| Figure 20: Design 3 of the shaft showing the tip of the three-lumen shaft that could incorporate all five functions..... | 29 |
| Figure 21: Expanded view of the peristaltic pump used to run the suction and irrigation for the MFSD | 33 |

| | |
|--|----|
| Figure 22: MFSD integrated buttons..... | 34 |
| Figure 23: PCB Layout (left) and 3D rendering of the printed circuit board (right) for the MFSD buttons | 35 |
| Figure 24: Rendering of the printed circuit board, push button caps, and header for the MFSD buttons | 35 |
| Figure 25: Integrated push button PCB (arrow) installed in the handle of Design V | 36 |
| Figure 26: Rendering of the printed circuit board for the control circuit | 37 |
| Figure 27: 3D rendering of the printed circuit board for the control circuit populated with the electronic components..... | 37 |
| Figure 28: End-view of the Design V shaft with the combined LED light and camera installed | 39 |
| Figure 29: End-view of the Design VI shaft without any electronics implemented | 40 |
| Figure 30: SolidWorks dimensioned model | 41 |
| Figure 31: Unshielded cautery element prototype with electrically isolating fiberglass tubing between the copper and nichrome wire..... | 42 |
| Figure 32: Setup using thermal camera for prototype development | 43 |
| Figure 33: Schematic of the second cautery element (secondary outer silicone sheath not shown for clarity)..... | 44 |
| Figure 34: Screenshot of the tablet user interface for parabolic flight..... | 51 |
| Figure 35: Arduino Nano..... | 52 |
| Figure 36: Side view of the flight hardware for parabolic flight. | 53 |
| Figure 37: MFSD in its holder pre-flight..... | 54 |
| Figure 38: Installed design development model of the final version of the 8mm leak-free trocar..... | 54 |
| Figure 39: Experimental layout for the stand-alone testing for the MFSD before flight..... | 59 |
| Figure 40: Overhead view of the flight hardware with the MFSD being used inside the surgical containment dome attached to a bleeding wound model | 60 |
| Figure 41: Side view of the flight layout that was used to test Design VI..... | 61 |
| Figure 42: Tip of the Design V shaft with the combined LED light and camera installed | 63 |
| Figure 43: External cord and the 3D printed enclosure to isolate the camera electronics. | 64 |
| Figure 44: Combined LED light and camera implemented into the shaft of Design VI..... | 65 |

| | |
|--|-----|
| Figure 45: Side view of the Design VI MFSD shaft..... | 66 |
| Figure 46: Showing the test of the original prototype that reached 122°C | 67 |
| Figure 47: Original cautery element in the fiberglass tubing intended to be implemented into the MFSD shaft | 68 |
| Figure 48: Tip of the new Design VI shaft. End view (left). Side view showing copper tip (right) | 69 |
| Figure 49: Test photo from Design VI of the MFSD. | 73 |
| Figure 50: Test photo from the original Ambu bronchoscope..... | 73 |
| Figure 51: Maximum temperature observed was 85°C for the low temperature cautery..... | 74 |
| Figure 52: Maximum temperature observed was 104°C for the high temperature cautery..... | 75 |
| Figure 53: Image showing the pre-flight testing, including the functioning LED light and camera shown on the Ambu monitor..... | 76 |
| Figure 54: Partially filled immersion dome during experimental flight with the MFSD inserted via leak-free trocar. | 78 |
| Figure 55: Full Block Diagram of LabVIEW code..... | 99 |
| Figure 56: Closeup of Master Cluster showing system variables | 100 |
| Figure 57: Close up of Data Queue creation | 100 |
| Figure 58: Close up of User Event Structure and State Machine | 101 |
| Figure 59: Close up of Visualization Loop | 101 |
| Figure 60: Close up of Data Saving Loop..... | 101 |

LIST OF TABLES

| | |
|-------------------------------------|----|
| Table 1: Design Specifications..... | 32 |
| Table 2: Cautery Test Results..... | 75 |

I. INTRODUCTION

The prospect of long-distance space travel is on the near horizon. One of the significant challenges will be medical management of the astronauts, particularly if surgery is ever required, which will be performed in microgravity and at great distances from Earth with little to no ground support. Since space and weight are at a premium in a spacecraft, adding additional equipment adds to the cost of a flight campaign, so small and compact medical equipment and surgical technology, perhaps novel technology created specifically for zero gravity, are of interest. This apparent need for surgical equipment and protocols that can be followed in reduced gravity are a necessary adaptation to the fundamental challenges created by a microgravity environment.

1.1 Microgravity Standard Practices

There are current standard practices and associated equipment developed for astronauts in zero or micro gravity related to non-medical related tasks. Some examples are the bungee systems used for exercise [1], the sleeping bag for adapted sleep [2], and even considerations for how cooking will happen in space [3]. Unfortunately, there is little to no research on specific tools and/or protocols for surgical and medical techniques that will be impacted by the restrictions created by microgravity.

For years, spaceflight providers have been creating plans to either complete extended missions to the moon [4-6], or even go farther than before to Mars [7-10]. While these sorts of long-term space travel missions are still in the planning stages, methods to provide necessary healthcare by the time the missions become reality need to be investigated so astronauts can receive proper medical care and be able to handle for any medical emergency that may arise.

1.2 Problem Statement: Multi-Functional Surgical Device

Due to an identified lack of surgical devices created specifically for use in microgravity, we want to develop a Multi-Functional Surgical Device (MFSD) that will accomplish five different functions in a form factor on the same scale as existing singular function medical devices (e.g., surgical suction wands). Specifically, a more compact multi-function device will be created to complete five commonly used functions in surgery: *suction*, *irrigation*, *illumination*, *visualization*, and *cautery*. The device should have similar efficacy to all the individual devices that complete the same function, while also being adapted to function in microgravity. Since most endoscopic-type medical devices have usable space inside the handle/grip, and there are existing examples of surgical instruments that have combined components, a modified wand could be created to take advantage of the extra space and add additional functionality. Our multi-functional device should perform the same functions as individual devices but integrated into a single handheld unit in a more compact form. This technology concept will enable efficient allocation of spacecraft storage space and during

surgery it will minimize delays during instrument exchange and prevent misplacement of individual surgical tools. Finally this development will be a positive step towards creating medical devices designed to accompany astronauts during long-term space travel.

1.3 Project Specific Aims

To accomplish the goals of the project, three specific aims were identified:

Specific Aim 1: Implement the final two functions of the MFSD, visualization and cautery.

- *Objective 1a: Identify potential materials for use in the device*
- *Objective 1b: Create each of the final functions*

Specific Aim 2: Establish functionality of the MFSD compared to the individual surgical devices

- *Objective 2a: Measure or identify normal performance values for each of the individual devices*
- *Objective 2b: Measure the normal performance values of the created surgical device*
- *Objective 2c: Compare the created surgical device performance values against the values of each of the individual devices*

Specific Aim 3: Test the functionality of the MFSD in microgravity

- *Objective 3a: Test the function of the MFSD in microgravity*
- *Objective 3b: Obtain data from each function of the MFSD during microgravity*

By accomplishing these three aims, the proposed study will create a novel technology sufficiently evaluated to confirm efficacy. It is expected that this project will demonstrate the adaptability of medical devices for extreme use conditions such as microgravity, while creating a valuable multi-functional surgical device that has the potential be useful for Earth-based procedures. Additionally, this device will begin to address some of the concerns of healthcare

in this particular extreme scenario and help to show these limitations can be overcome for the prospect of long-term space travel.

II. BACKGROUND

It has been predicted that by 2040, human-occupied space stations/habitats could be created on the moon and Mars, we will have international space stations orbiting other planets in our solar system, and space travel will be a routine activity [11]. These activities include the continued development and maturation of commercial space travel [12]. There are several primary challenges in the environment of space including microgravity, radiation, extreme temperatures, and pressures, and when occupying celestial bodies, a whole new physical and chemical environment compared to Earth [11-13]. Considering these challenges, a new field of medicine was created with the idea of long-term space missions in mind: *space medicine*. This budding field can be defined as “the practice of all aspects of preventative medicine including screening, health care delivery, and maintaining human performance in the extreme environment of space and preserving the long-term health of space travelers.”[14] This field needs to be highly collaborative between physicians, engineers, mission planners, and other experts to create adequate space medicine techniques and technologies to enable successful space exploration [15].

In 2017, the IMM of the NASA Human Research Program included a list of one hundred possible medical conditions that could happen during spaceflight.

Off of that list, 27 of them required surgical intervention [16]. Since the creation of this list, space medicine, specifically space surgery has increased in popularity amongst researchers [16-21], but it still woefully underdeveloped and requires much more research and innovation to reach the point where surgery can be completed in space.

Although there is a rigorous medical evaluation each potential astronaut must undergo [22], the crew must still be prepared to treat accidents and illnesses that are unable to be foreseen or prevented by these evaluations [11, 15, 23-26]. These events will likely impact mission objectives greatly and could leave the crew severely crippled [16, 24]. Some of these possible medical events could include blunt and penetrating traumas, chemical contamination and burns, minor injuries, and other surgical issues [24]. With long term space missions there must be a doctor on board that must be competent in all fields, including surgery [11, 26, 27]. The crew doctor and the rest of the crew will be on their own to ensure the safety of the crew since there will be significant communication delay [15, 23]. Currently, the sick and injured on the ISS can be stabilized and returned back to earth usually within twenty-four hours [27, 28]. However, with missions to the moon and Mars, this return time dramatically increases, making an evacuation problematic [15, 16]. It was estimated that returning from the moon could take three to four days causing the crew member to have to suffer for a long time and could worsen their condition greatly [16, 27, 29]. For Mars it is predicted that the one-way trip would take almost nine months, meaning medical evacuation would not be an option [16, 26, 28, 29].

Although telemedicine and robotics were thought to be a good option, there are time delays, and space and weight concerns that make this not a viable replacement for a surgeon providing the surgical care [13, 15, 26]. It has been shown that the communication delay from Mars can range anywhere from four to forty-five minutes, depending on the planet's location [15, 16]. The other major issue is the volume and weight of a robot capable of assisting in space surgery [16]. The current size and weight of these robots make it not feasible to be brought along in the spacecraft since volume and weight are severely limited [16]. Finally, robotic surgery can only add to, not replace the surgical skills of the operator since controlling remotely is not an option due to the communication delay [16]. Overall, these negatives make the use of a surgical robot almost impossible and not helpful to the mission.

Since these medical and surgical challenges exist and there is no alternative for traditional healthcare, novel technologies will need to be created to accomplish the wide range of space medicine applications [15]. This includes smaller multi-functional equipment that will help to save on volume and weight on the spacecraft [13, 15, 16, 26, 29]. Since there is no gravity to prevent blood and other particulates from floating away, laparoscopy would seem to be a more attractive alternative compared to open surgical procedures [23]. Completing any surgery in zero gravity will be challenging, but surgical instrument accommodations and augmentations could compensate for the degradation of surgical performance [23, 25]. All of these concerns create an obvious need for a

compact multi-functional surgical device that is capable of completing laparoscopic surgery and treating external wounds.

2.1. Problem Statement

Due to the increased popularity in long-term space missions and commercial spaceflight, medical care will need to be provided by the crew of these long-term missions. Due to the communication delay and weight and volume constraints, telemedicine and robotic medicine are not an option for these extended space missions. Telemedicine will be limited by significant communication delays caused by ever increasing distances from Earth [30], and surgical robots would be too large and heavy to be feasible on a spacecraft making an extended mission. In addition, this robotic system would still require an operator since remote operation would not be an option due to the previously mentioned communication delay.

Keeping volume and weight constraints in mind, this creates the need for a compact multi-functional surgical device that could be utilized in zero gravity on these long-term space missions, if necessary. This device could incorporate common surgical functions and would be easily usable by the crew medical officer. Since dexterity is already reduced in zero gravity [31], this device would be created to be as simple and intuitive as possible.

2.2. Existing Multi-Functional Medical Devices

Most current surgical devices complete a singular function, but multi-functional devices are available. Although there are a handful of devices that

exist, they are not commonly used based on personal observation and conversations with medical professionals.

One device is the ENDOPATH Electrosurgery PROBE PLUS II (Ethicon, Inc., Raritan, NJ, Figure 1). This device combines suction, irrigation, and monopolar cautery functions. This device has a diameter of 5mm and is for laparoscopic use.



Figure 1: The ENDOPATH Electrosurgery PROBE PLUS II

A second example of a multifunctional device is the Bovie® Suction Coagulator (Symmetry Surgical, Antioch, TN, Figure 2). This laparoscopic device combines suction and monopolar cautery.



Figure 2: Bovie Suction Coagulator

A third multi-functional device is available from Medtronic. The Aquamantys MPR Bipolar Sealers (Medtronic, Inc. Dublin, Ireland, Figure 3) provides irrigation, illumination, and bipolar cautery and is only compatible with open surgical procedures.



Figure 3: Medtronic Aquamantys MPR Bipolar Sealers

There still remains a gap in available technology for a laparoscopic all-in-one device that accomplishes suction, irrigation, cautery, illumination, and visualization. Especially if this can be accomplished using a general instrument size that is already commercially used.

2.3. Cautery

Cautery is “the action of burning body tissue using heat or a chemical, to stop an injury from bleeding or getting infected, or to remove harmful cells. Cautery can be used to remove unwanted tissue, create cuts in the tissue, burn and seal blood vessels, and can help reduce or stop bleeding using coagulation.

In a multi-functional device, dual temperature cautery would seem to be an attractive additional function due to its multiple functions and versatility in different procedures.

2.2.1 Electrosurgery

The most common type of cautery used clinically is what is called electrosurgery, where a modulated alternating current is applied to the tissue at different rates to create the desired reaction [32]. Electrosurgery devices are configured as either monopolar or bipolar devices. Monopolar refers to current leaving the active device tip and exiting through a grounding pad on the patient. Bipolar refers to a dual electrode configuration, where current flows through one electrode and back through the secondary electrode. While these are the most common devices, they use alternating current, which can be problematic for a spacecraft at high power and possibly create electromagnetic frequencies that could influence board equipment. In addition, these devices can cause severe shocks and burns due to the fact that the current must run through the patient [33, 34]. Due to these limitations, creating a cautery mechanism that implements electrosurgical techniques was not considered.

2.2.2 Thermal Cautery

Electrocautery, also referred to as thermal cautery, is the process where either a direct or alternating current is applied to a resistive metal electrode, which then creates heat. This heat can be used to stop bleeding and cut tissue, like electrosurgery [35]. Unlike electrosurgery, thermal cautery does not require a

grounding pad, and does not push electrical current through the patient, making it a safer alternative to electrosurgery [36, 37]. In addition, since thermal cautery can be created with the choice of direct or alternating current, a reduction of EMF could be achieved with thermal cautery compared to electrosurgery.

2.4. Multifunctional Surgical Devices: Implications

Despite a focus on medical and surgical care for long term space travel, the technology proposed in this project will also have implications for earth-based healthcare [36]. Since most instruments for laparoscopic surgery are single function, this adds time in surgery due to instrument exchange [35]. This can add an additional 10-30% of total time due to the instrument exchange, which could compromise the safety of the patient [11]. The creation of a multi-functional device would help to reduce the time spent during instrument exchange and could help to better patient outcomes.

2.5. Previous Developments

2.5.1 Aqueous Immersion Surgical System

Through funding awards from the NASA Flight Opportunities Program, the University of Louisville, Carnegie Mellon University, and Cornell University worked in tandem to create technology to assist with performing surgery in space. Specifically, two different Aqueous Immersion Surgical Systems (AISS) were developed. The goal was to create a dome that would attach to the skin over a wound site that could be filled with irrigation solution (e.g., sterile saline) to keep tissues hydrated and to provide therapeutic tamponade to stop bleeding.

The University of Louisville aimed to develop a rigid dome, while Carnegie Mellon University and Cornell University worked on the creation of a compliant dome. These domes when filled with fluid would help to control bleeding, clean the wound, and help to maintain a clear visual field during surgery. These systems include a series of pumps, pressure transducers and flow probes to control the pressure feedback and accomplish a few automated surgical tasks. The University of Louisville AISS also implemented an early prototype version of the MFSD (Design IV) to demonstrate a surgeon completing some tasks and demonstrate how surgical tools could be used without leakage. This AISS configuration was also proven effective during active use in a suborbital space flight (Figure 4 and Figure 5).



Figure 4: Side view of the University of Louisville suborbital AISS experiment, showing the Design IV MFSD that was implemented for suborbital flight.

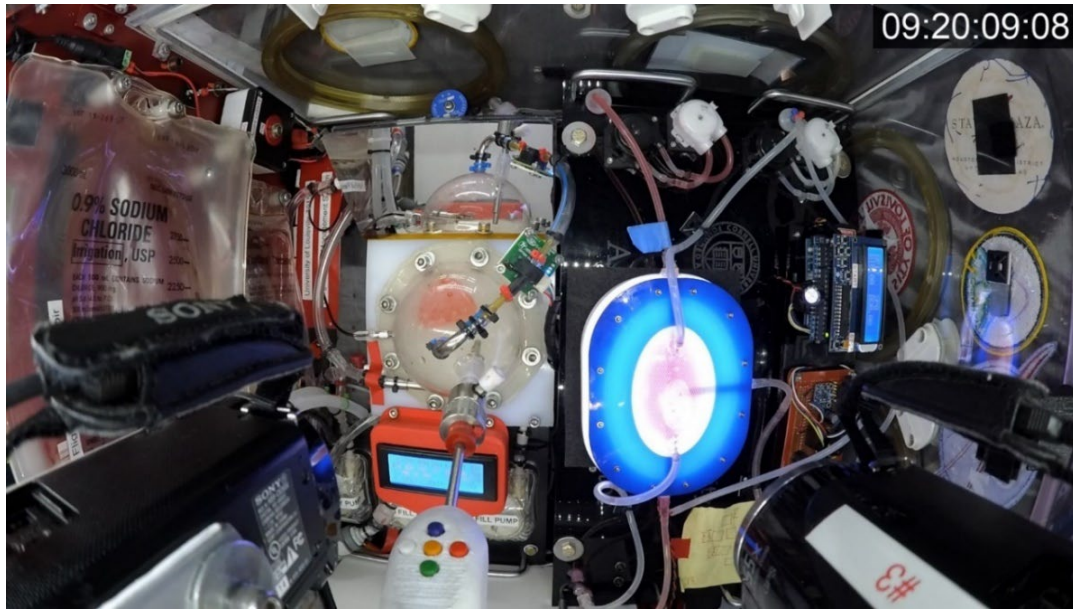


Figure 5: Overhead view of the University of Louisville and the Carnegie Mellon/Cornell University suborbital AISS systems in the Suborbital Glovebox during suborbital flight

2.5.2 Surgical Immersion Dome

The surgical immersion dome (Figure 6) is a transparent dome made from vacuum formed polycarbonate and is essentially the heart of the AISS system that was previously described. The purpose of this device is to create a wound isolation dome that could be attached to the skin and cover an exposed wound equipped with easily connected surgical fluid ports, the surgical immersion dome was envisioned as a technology to perform several functions: to cover a wound to prevent contamination of a spacecraft with blood and/or tissue debris; to keep the wound clean; to reduce intraoperative blood loss; and to maintain adequate visualization of the operative field. The shape of the dome has been designed to allow for the best visualization and optimal filling. Since fluid behaves differently in zero-gravity, the predominant force is surface tension which causes liquids to

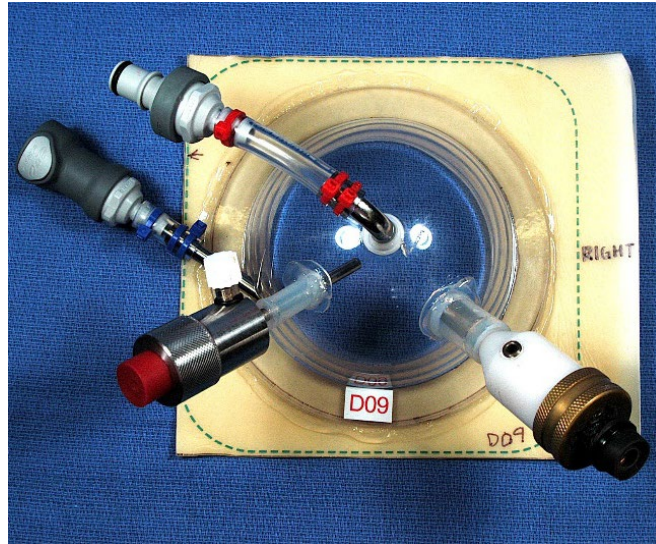


Figure 6: Surgical Immersion Dome with 3mm and 8mm Leak-Free Trocar inserted.

stick to the interior surface and potentially create air pockets during the filling stage which would block the visual field. The optimal dome shape was experimentally determined to be the hemispherical dome shape, as opposed to other conical and concave shapes that were also evaluated. This was determined based on the filling performance and the consideration of visual distortion and ability to manipulate the surgical instruments. These domes have been able to be attached to a DuoDerm CGF and 3M™ Ioban™2 dressing in order to adhere to human skin completely using a material that is biocompatible. These domes were also proven effective during active use in both parabolic and suborbital space flights (Figure 7).



Figure 7: Eight surgical immersion domes with the attached loban and Duoderm seal laminate, filling and emptying ports, and the surgical instrument ports incorporated into the dome.

2.5.3 Leak-Free Trocars

For space surgery capabilities, it is necessary to create devices that are leak-free to reduce debris and fluid that may contaminate the interior of a vehicle experiencing zero gravity. Current endoscopic trocars are not designed to be leak-free [38], meaning that it was necessary to create a set of trocars that do have a leak-free design. A set of leak-free trocars were made of various sizes to interface with the surgical immersion dome and allow for leak-free use of surgical instruments when the dome is full. This technology incorporates two multi-leaflet valves and a dual-tapered diaphragm end cap seal that can maintain pressure up to 100 mmHg for both air and fluid insufflation (Figure 8). These trocars were also proven effective during active use in both parabolic and suborbital space flights.



Figure 8: Isometric rendering of a 5mm Leak-Free Trocar.

2.5.4 Fluid Management System

The fluid management system provides control over all of the fluid functions of the AISS. Configured for either manual or automated control, the electronics enables the filling, purging, emptying, and modulation of pressure in the AISS. There are inputs from an in-line, absolute pressure sensor, an inline flow probe, an optical sensor to monitor the air/fluid interface at the roof exit port of the dome, temperature sensors (suborbital version only), and an integrated accelerometer to monitor g's during parabolic and suborbital flights. This system supports and enables the functionality of the surgical immersion dome to provide the possibility to perform minor surgeries in zero gravity. The system was proven effective during previous parabolic flights, and a fully automated suborbital flight on Virgin Galactic's SpaceShip2 in May 2021, and on numerous parabolic flights where the dome and overall system functionality was evaluated.

2.5.5 The Experiment Glovebox

The experiment glovebox (Figure 9) was created with the idea of suborbital and parabolic flight in mind. All flight providers require secondary containment to prevent contamination of the air/spacecraft by liquids, solids, or particulate that could be released by an experiment. The primary design goal of the glovebox was to provide this secondary containment, but also allow for it to be reusable and customizable for different types of experiments. The glovebox is a transparent polycarbonate canopy with a base plate and back plate made of 6061 anodized aluminum. It has three sets of arm access ports inspired by neonatal incubator canopy units. These access ports allow for investigators to work with the side doors sealed during ground, parabolic, and suborbital testing. There are two external electrical connections on the front of the glovebox



Figure 9: Experiment glovebox with two arm access ports open

connect to feed through ports in the bottom of the glovebox to bring electricity provided by the flight providers to the payload. Both side doors have hinges that open near 180° to allow for access inside the glovebox for experiment installation and maintenance. The glovebox is the size of two stacked ISS stowage containers (18.5" x 23" x 21.5") and has been designed to be able to interface with current suborbital research flight spacecraft (e.g., Blue Origin and Virgin Galactic). The glovebox accommodates a pair of internal modular experiment boards each with a maximum size of 10" x 17".

2.5.6 Modular Experiment Board

The glovebox has integrated mounts for experiment boards that could be customized and changed for quick exchanges between experiments. Two different experiments can be installed into the glovebox if size constraints are met. This configuration was demonstrated during the suborbital flight in May of 2021 on Virgin Galactic's SpaceShip2 at their Spaceport America launch facility. The two versions of the AISS systems were demonstrated during this flight; the compliant dome created by Carnegie Mellon University and Cornell University, and the rigid dome created by the University of Louisville.

2.6. Previous MFSD Developments

2.6.1 Fall 2016 Capstone

The beginning of the MFSD started during an undergraduate Capstone project in the Bioengineering Department at the University of Louisville in 2016. The goal was to create an early concept of the Multifunctional Surgical Device. This iteration will further be referred to as Design I of the MFSD. Due to the time constraints, this original proof-of-concept device included suction, irrigation, and illumination, as the team deemed those to be the most important functions. The final design (Figure 10) was a clamshell handle closed with set screws, with five 12 mm buttons that worked the three functions of the device. The suction and irrigation portion were run off of one peristaltic pump and two solenoid valves (Figure 11). Illumination was accomplished by adding a fiber optic light to the outside of the shaft of the MFSD.



Figure 10: MFSD Design I prototype

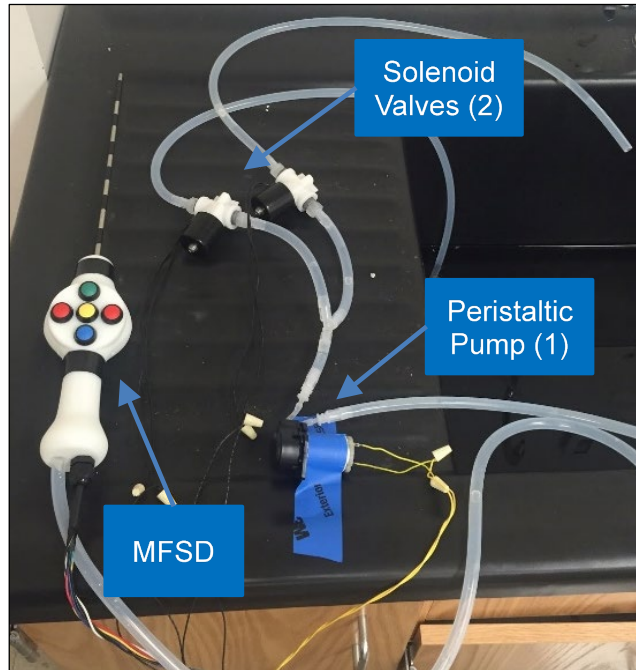


Figure 11: The fluid circuit for Design I of the MFSD

Although the functionality was successfully demonstrated on this device, there were a few improvements that could be made. The first was the fiber optic did not provide adequate illumination since the fiber optic was so small. A larger light source would need to be considered to provide better illumination. The next was that the handle was too large and difficult to maneuver. The thumb-activation functions affected the ergonomics of the device. It was determined that reducing the diameter of the handle and changing the buttons to be fingertip activation would help to increase the comfort and functionality of the device. The last negative was that the pump could not create a fast enough flow to reach thresholds that were suitable for endoscopic procedures. The pump was able to reach about 1 mL/sec (60 mL/min), but the goal was 1 L/min. This could be

remedied with a faster pump, and larger shaft area. All of these notes were considered when Design II was being created.

2.6.2 Summer 2018 MEng Thesis

During the summer of 2018, designs II, III and IV were created by a previous student. Each of the designs incorporated suction, irrigation, and illumination functions, but were dramatically different regarding the handle, shaft, and buttons. For Design II, the thumb-activation style was abandoned in favor of switching to finger-tip activation. The large buttons on Design I were difficult to use and made the handle of the device very large. Design II (Figure 12) included custom pushbutton caps and a smaller diameter handle. This provided for a more comfortable design and allowed for greater control of the device. This handle was about 6 inches in length, and 1.6 inches wide at the widest point of the handle. It had two internal clips where the shaft would attach to the handle, and then the



Figure 12: A rendering of Design II of the MFSD.

shaft would come out the tip of the handle to add additional stabilization. This handle was attached using 6 #2 x 0.5" self-tapping screws. The handle was 3D printed and tested for comfort, but no electronics were implemented.

While Design II was a drastic improvement compared to Design I, Design III realized a more subtle change (Figure 13). The rounded edges in Design II made it difficult for the user to stabilize the device. This led to the major difference in Design III. Design III incorporates flat sides on the widest part of the handle to help the user stabilize the device better. The handle design did not change in length, but the internal shaft attachments were moved forward. This made the overall length of the device slightly longer, without changing handle size. This increase in length also made the device more compatible with the leak-free trocars. In addition, the six set screws were reduced to four due to the

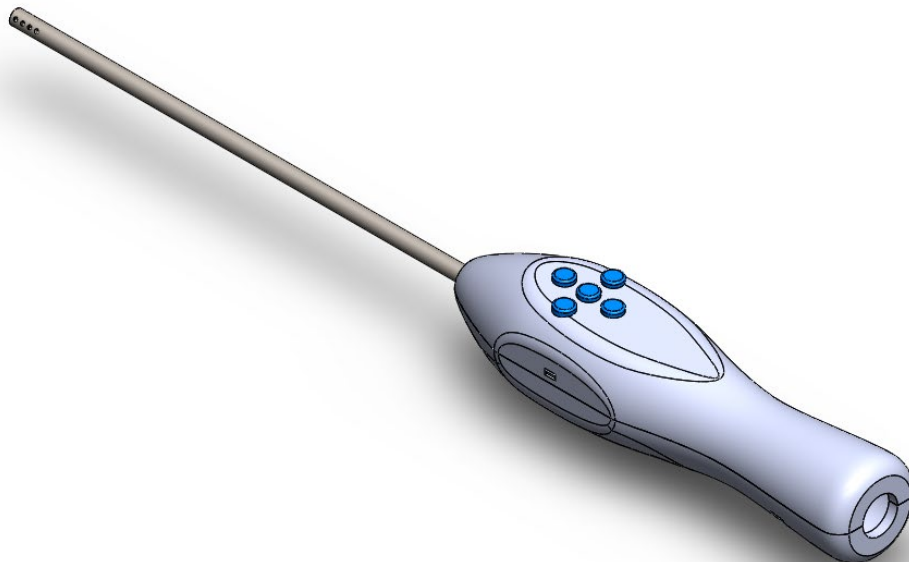


Figure 13: A rendering of Design III of the MFSD

addition of snap-fittings in the handle. The handle was 3D printed and tested for comfort, but no electronics were implemented.

Design IV was the final design created and evaluated during the summer of 2018 (Figure 14). This handle was smaller in both length and width compared to the two previous designs. The handle shaft was reduced to five inches in length and the width was reduced by another $\frac{1}{4}$ inch. The flat sides were retained to assist with the stability of the device. This created the most comfortable and maneuverable device to date. The snap fittings were abandoned, and 4 #2 x 0.5" self-tapping screws were used to attach the two sides of the handle. Lastly, small mating tips were added to the outer edge of the handle to assist in assembly and reduce the likelihood of water leaking out of the handle. A small threaded standoff was added to the end of the handle as well to assist in integration into the



Figure 14: A rendering of Design IV of the MFSD

Glovebox, however, this does not serve any other purpose. An exploded view of Design IV is shown in Figure 15.

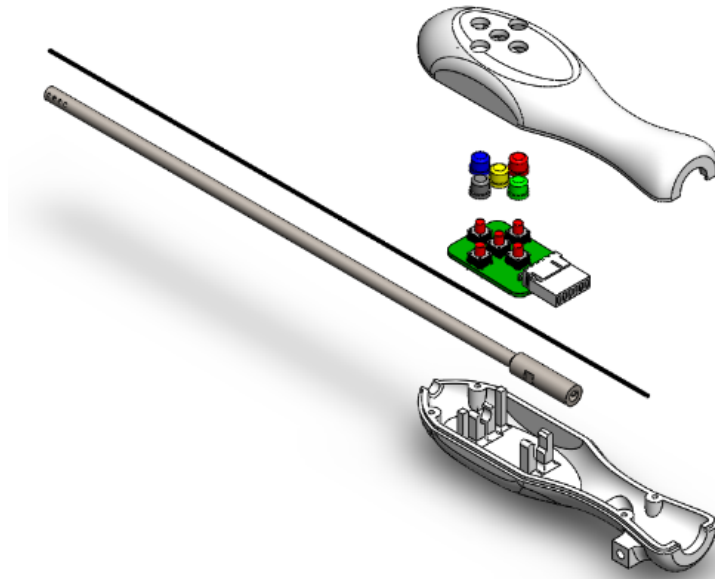


Figure 15: An exploded view rendering of Design IV of the MFSD

Since Designs II, III, and IV incorporated suction and irrigation (fluid) and illumination (visualization) functions, the shaft design (Figure 16) had two lumens. There was one smaller circular lumen that housed the fiber optic light source, and a second crescent shaped lumen where the irrigation and suction would flow through (Figure 17). This shaft had an external diameter of 5mm. This decision was made so that this device could be used with commercially available trocars and to mimic the size of current endoscopic medical devices. This shaft was 3D printed from 316L stainless steel by Protolabs through direct metal laser



Figure 16: 3D model of shaft Design IV of the MFSD (Length = 10.5in)



Figure 17: 3D model showing tip of the shaft for the Design IV of the MFSD

sintering [38]. In addition, small holes were added to the side of the tip of the shaft to prevent clogging and allow for multiple areas of suction.

This final design was put through multiple benchtop tests and flight tests to prove functionality of the device. It was proven to be leak-free, that the three implemented functions worked adequately, and was comfortable to use and maneuver. Despite this, there were some limitations in this design. The handle was not completely waterproof to external water, since water could leak in via the holes where the pushbuttons are, and the connection at the bottom of the handle where the electronics left the handle. A second limitation was in the lack of mechanical testing, although there was no indication of breaking during the benchtop testing, more rigorous testing like failure testing could be completed to

insure the strength of the shaft, handle, and their attachments. A third limitation is related to sterilization. Due to the complexity of the device, it is difficult to sterilize the device and components, especially during the assembly process. Ethylene oxide sterilization would be an appropriate process, but it is not always available.

2.6.3 Fall 2020 Capstone (Cautery Prototype)

In addition, there was a follow up capstone project completed by three Bioengineering students (Caitlin Howard, Kayla Montgomery and Sienna Shacklette) during the Fall of 2020 that worked on improving the MFSD. This project focused mostly on the proof-of-concept for the implementation of cautery, and how the handle and shaft would have to change in order to accommodate the cautery function. There were three primary outcomes at the end of this capstone project: 1) determining which type of cautery would work best for implementation in the device specifically for a space surgery application, 2) creating a proof of concept for the cautery element itself, and 3) creating preliminary designs for new shafts that accommodate the shaft with cautery implemented.

Multiple modes of cautery were researched, and a small presentation was created on each of the different types and their pros and cons. After this presentation, it was decided with the group members and the mentors that thermal cautery would likely be the best course of action due to it being safer than other methods. Namely, it could be accomplished using a DC power supply with little electromagnetic interference and appeared to be the easiest to implement. Thermal cautery could be achieved by sourcing adequate current

through a resistive element to create enough heat to burn tissue. The current and temperature was not documented at this time, only the visual observations were made.

A basic proof of concept circuit was created and was tested by applying heat to a small piece of bacon. It was determined that incorporating a heating element into the device shaft was not possible. References on how to create a cautery device were not readily available, so inspiration was gleaned from other devices that use similar physics. This circuit consisted of a 9V battery, two alligator clips with stranded copper wire, a piece of fiberglass fabric tubing, a thick piece of copper wire and nichrome wire (Figure 18). This was accomplished by putting the thick piece of copper wire inside the fiberglass fabric tubing. This tubing was then wrapped in nichrome wire, and each end of the nichrome wire

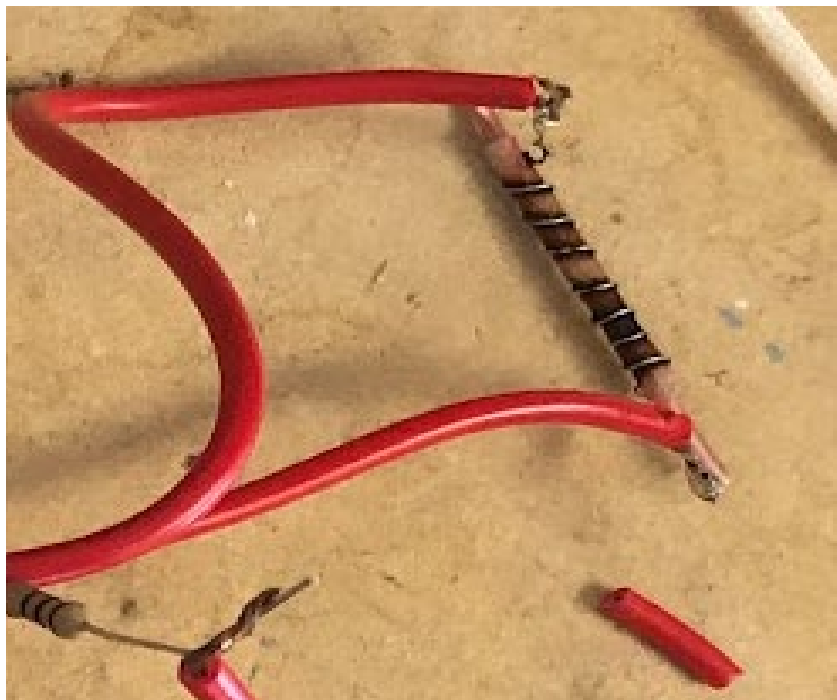


Figure 18: Heating element, showing the copper, fiberglass tubing, and the coiled nichrome wire

was attached to the stranded copper wire. The alligator clips were then attached to the 9V battery, and this circuit generated enough heat to burn biological tissue (bacon was used) (Figure 19).

For the third accomplishment, three shaft designs were created as a preliminary design for what the new shaft could look like. Design 3 was the final design as each was an improvement on the last. This design included three lumen: one for the cautery element, one for the combined camera and LED light, and one for the suction and irrigation pathway (Figure 20). Due to the increased space needed for all three lumens, this shaft was increased to 7mm in diameter. Previous designs have always been 5mm in diameter. The 7mm diameter was still a clinically relevant size, since there are existing 7mm and larger endoscopic devices.

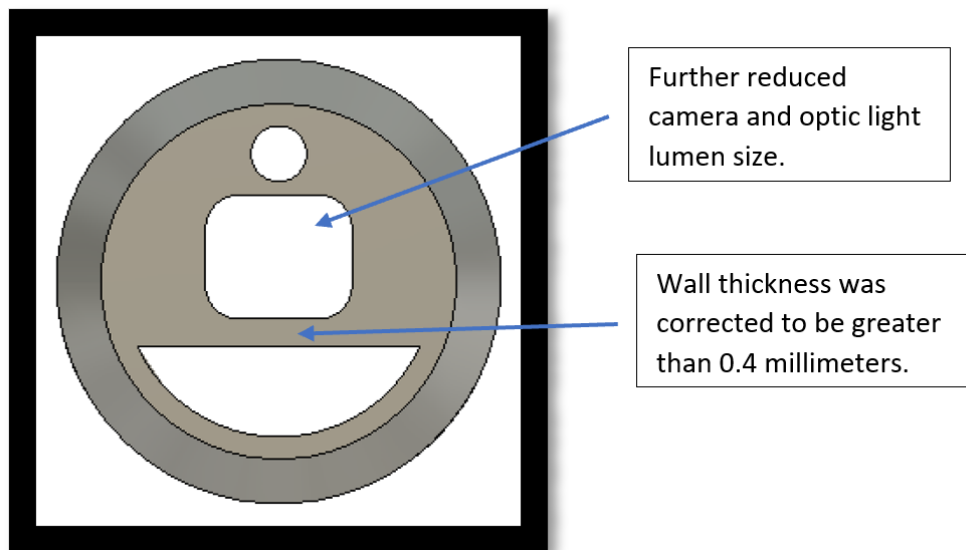


Figure 20: Design 3 of the shaft showing the tip of the three-lumen shaft that could incorporate all five functions

III. MATERIALS AND METHODS

3.1. Design Criteria

3.1.1 Objectives

As an improvement on previous designs, the major goals that needed to be achieved was the implementation of the visualization and cautery functions. It has been shown in previous designs that the suction, irrigation, and illumination were possible, but there was no concrete work on the addition of a camera and heating element. With keeping in the size constraints, these two functions would need to be added to include all five functions. In addition, there were a few other improvements that needed to be addressed. One of those being the attachment between the clamshell handle and the stainless-steel shaft. The previous prototype had clips on the inside that would routinely break and took away space inside the handle that was needed for additional electronic components and printed circuit boards to be added inside the handle. Ultimately, with those improvements, the aim was to keep the device very similar in size and functionality overall. The device would need to be tested that all five functions were able to be used to the standards of current medical devices, worked well with a control circuit, was intuitive in its function, and was still comfortable to use by the investigator.

3.1.2 Technical Specifications

In addition to the design and functionality criteria discussed above, there are a few technical specifications that were also identified. These technical specifications include device size and weight, shaft diameter, fluid flow rate for suction and irrigation, illumination strength, visualization clarity, and cautery temperatures.

Overall, the device weight, device size, and shaft diameter need to remain of similar size and shape from previous designs in order to remain comfortable to use and easily maneuverable. In this project, version IV of the handle was deemed to be of a satisfactory size and only adjustments to accommodate an adjusted shaft diameter were made.

The target shaft diameter should match the leak-free trocar orifice sizes, while accommodating the internal functions (cautery function, camera function, and lumen for fluid flow).

When it comes to the suction and irrigation function, the goals were to have the suction and irrigation lumens be able to flow from both sides without clogging or leaking at higher pressures. There is a goal temperature for cautery, but it can range depending on the tissue type, environment, and desired effect. For this case, it needs to be hot enough to be effective, but not too hot that it could cause damage to the patient or the user. Based on research, it was determined that the current goal temperatures for the dual temperature cautery

would be 90°C and 120°C for the low temperature and high temperature cautery, respectively.

Table 1: Design Specifications

| | |
|-----------------------------|---------|
| Wand Handle Diameter | 1.35 in |
| Temperature (Low) | 90°C |
| Temperature (High) | 120°C |

3.2. Device Hardware

3.2.1 Fluid Components

The MFSD fluid system consists of two peristaltic pumps, ¼” silicone tubing, a Y-connector, a fluid source bag, and a fluid waste bag. The shaft of the device shares a small section of ¼” silicone tubing that is then split by the Y-connector into the suction and irrigation tubing. The directionality of the tubing is dictated by the pumps itself. The irrigation side will go from the fluid source bag, through the peristaltic pump and out the tip of the device. The suction side will go from the tip of the device, through the peristaltic pump and into the fluid waste bag. By using the two peristaltic pumps, they act as valves when not being used. This keeps the waste from being pushing down the irrigation line, and the irrigation solution from being pushed down the suction line. The tubing attached to the shaft of the device was glued and sealed in place to keep any sort of pulling or separation from causing fluid to leak into the inside of the handle. A cable tie was also used Any fluid in the handle could cause issues with the printed circuit board, and this extra glue on the attachment will prevent this from happening.

3.2.2 Peristaltic Pumps

In endoscopic surgeries, the flow rates should be consistent and must provide adequate suction and irrigation without clogging or leaking. Additionally, using the peristaltic pumps allows for solenoid valves to be eliminated, since the peristaltic pumps act like a valve when not being used. The 12V peristaltic pump chosen (Honlite Industrial Co. Ltd., China, exploded view in Figure 21) provides approximately 1 L/min of flow and interfaced well with the ¼” silicone tubing.

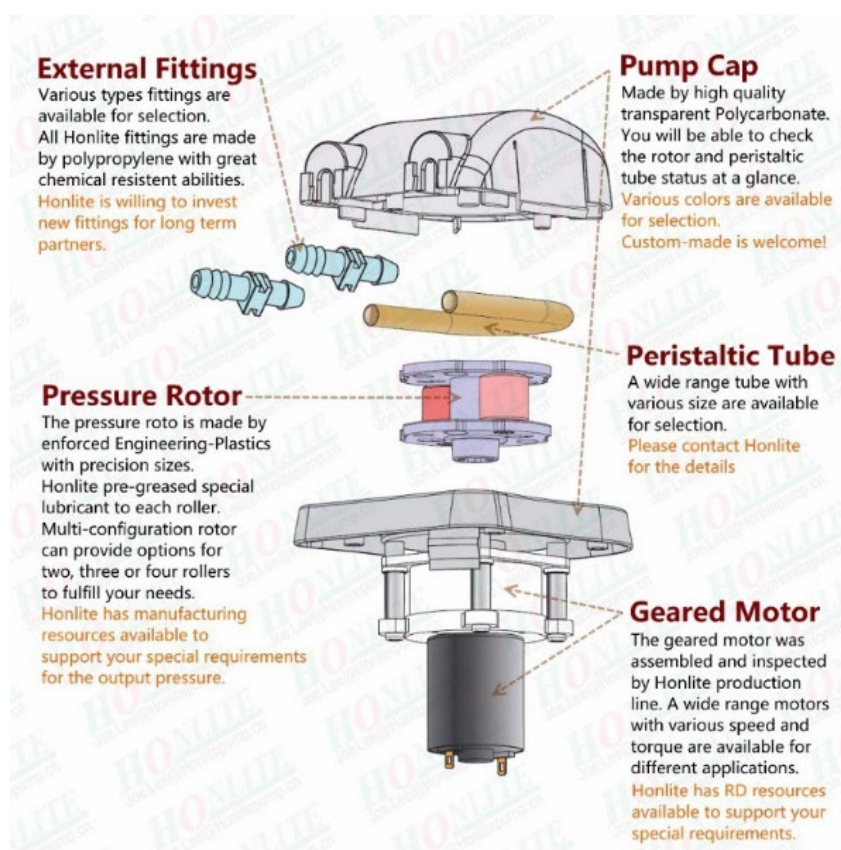


Figure 21: Expanded view of the peristaltic pump used to run the suction and irrigation for the MFSD

3.2.3 Button Switch Configuration

The button switch configuration (Figure 22) was unchanged from the previous design version. The buttons were small enough to allow for fingertip control, and the printed circuit board with the five button switches was reliable. This allowed for compact circuit board design inside the handle of the device (Figure 24) and allowed the device to remain comfortable to hold and easy to use.



Figure 22: MFSD integrated buttons

3.2.4 Button Switch Circuit Schematic

The button switch circuit board was unchanged from the previous design version. The PCB layout and top-down 3D rendering are shown in Figure 23. The circuit board fit well inside the handle, interfaced with the 3D printed pushbutton caps well, and was reliable. This simple design has each of the five button switches connected to a single 5V power source. These all attach to a six-pin header, that can attach to the external control system to turn on the necessary electrical components.

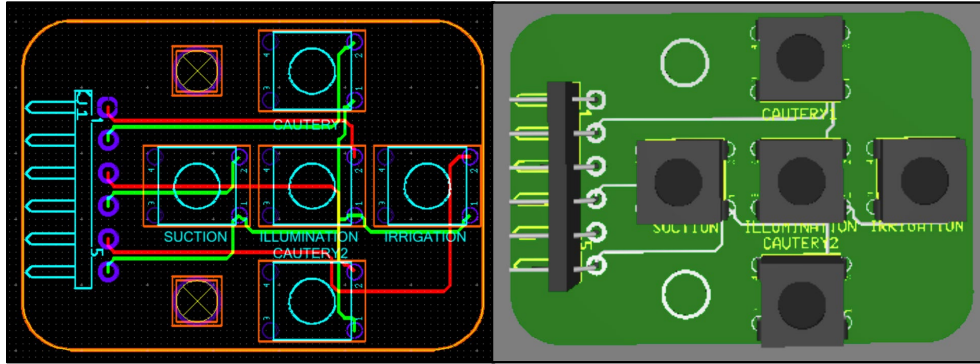


Figure 23: PCB Layout (left) and 3D rendering of the printed circuit board (right) for the MFSD buttons

3.2.5 Pushbutton Switch Caps

Since the design of the clamshell handle button spacing did not change, the previous 3D printed button caps for the tactile switches were used (Figure 24). The size of the buttons was adequate and since the handle did not change drastically in design, the device would still be worked with fingertip control. Since there was no change in design, the buttons were installed in the device by placing them in the holes in the handle. The pushbutton PCB was placed inside

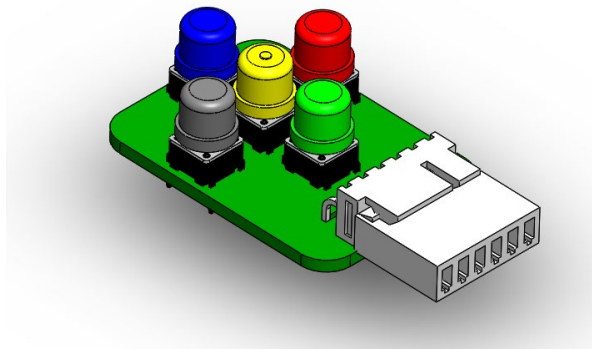


Figure 24: Rendering of the printed circuit board, push button caps, and header for the MFSD buttons

the buttons and screwed down to keep the buttons in place (Figure 25). The buttons were able to be integrated and they were confirmed functional.

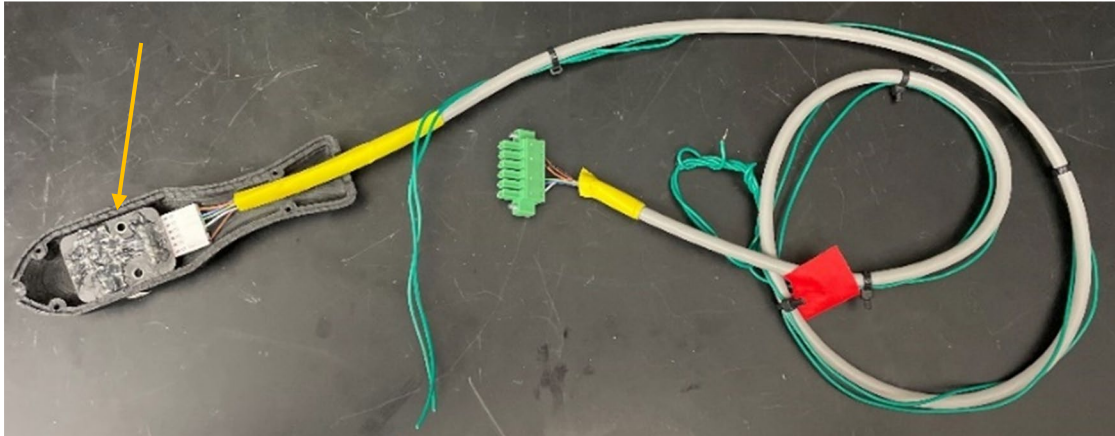


Figure 25: Integrated push button PCB (arrow) installed in the handle of Design V

3.2.6 Control Printed Circuit Board

In addition to the circuit board for the button switches, another a printed circuit board was created in order to control all of the additional functions of the MFSD (Figure 26). This printed circuit board was designed in Altium Designer (V 23, Altium Limited, La Jolla, CA) and was fabricated by JLCPCB (JLPCB.com, Shenzhen, Guangdong, China). This PCB incorporated an Arduino Nano microcontroller, and the other necessary electronic components to run the functions of the MFSD, the other flight components, and interface with the user interface on the tablet controller (Figure 27).

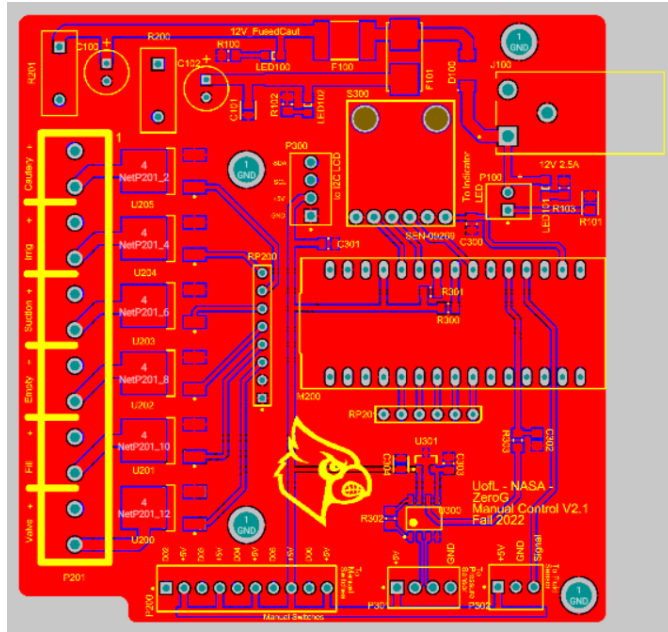


Figure 26: Rendering of the printed circuit board for the control circuit

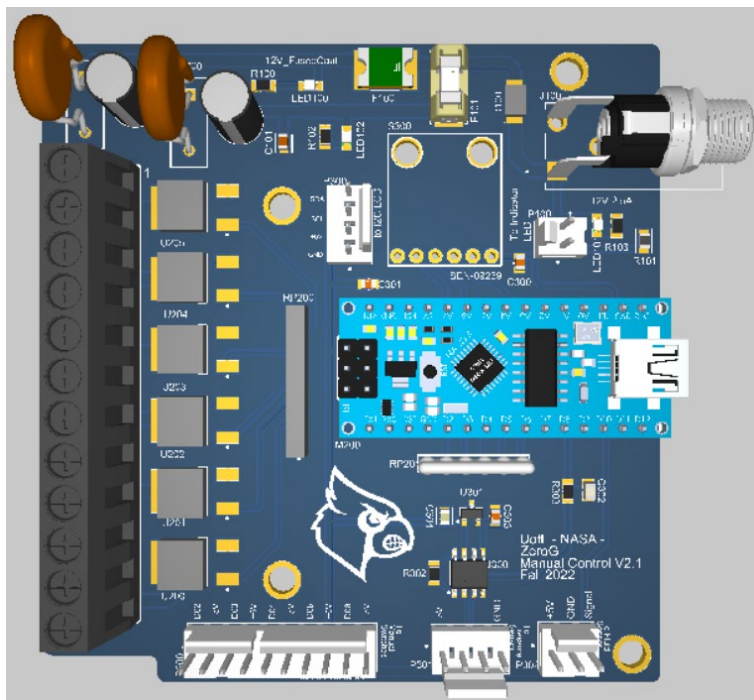


Figure 27: 3D rendering of the printed circuit board for the control circuit populated with the electronic components.

3.2.7 Combined LED Light and Camera

In order to establish the visualization and illumination function, it was thought that the best way to do so was to find an existing combined camera and LED component to add to the design. It was thought that this would help to save space and could provide better illumination since the camera and light would be right next to each other. After some research searching for independent light and camera components, it was found that the combined camera and light from an aScope 4 disposable bronchoscope (Ambu, Ballerup, Denmark) would be an adequate light and camera. Since these bronchoscopes are used currently in medical procedures, it would be a bright enough light, and a clear enough camera to fulfill the function we needed. Since the bronchoscopes are single use, after the assigned use they could be decontaminated and dismantled, and the camera could be cut out with relative ease. The bronchoscope cameras are set in some form of plastic potting that was able to be filed down to the desired shape and reduce some of the size of the camera. This allowed for the combined camera and light source to be about 4mm at its widest point. Other independent light and cameras found online ranged from 5-9mm. The bronchoscope camera was much smaller and was a safer option since it was already used in medical devices. The camera itself, the driving PCB, and the connector cable to the bronchoscope monitor were able to be removed from the body of the bronchoscope and implemented into the MFSD. The wires from the camera to the PCB were disconnected in order to put the camera in the shaft. The camera was glued into the end of the shaft in its assigned spot, and sealed from both

ends of the shaft to prevent liquid from leaking onto the camera and its wiring. The wiring from the camera was soldered back onto the PCB in the same spots they were taken from. The small PCB that drives the camera and light was integrated into the handle of the device. Once the handle and shaft attachment were redesigned, there was more room in the handle for the electronics to be added in. This PCB rested under the pushbutton circuit and was glued into the 3D printed handle. The cable was brought out the end of the handle and attached

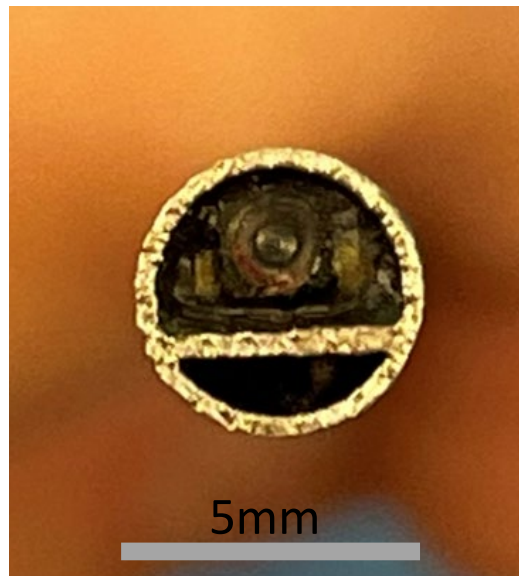


Figure 28: End-view of the Design V shaft with the combined LED light and camera installed

to the other wiring. This cable would go into the existing Ambu monitor to show the video and to power the LED light source. The light and camera were able to be implemented and functionality was established.

3.2.8 Suction and Irrigation Wand

Due to the nature of the shaft of the device, it was decided that the creation of a custom multi-lumen device was required. This will allow a custom

diameter, and the separation of each of the lumens of the device to stop the interaction of electronics and fluid. The shaft design was 3D printed by direct metal laser sintering the Advanced Manufacturing Lab at the University of Louisville (Figure 29). This 3D printing allowed for a variety of choices of materials and had high resolution that could create the unique shapes and thin walls of the shaft. The shaft was printed from 316L Stainless Steel due to its strength, resistance to corrosion and biocompatibility. The outside of the shaft was sanded to create a smoother finish and allow for more comfort to the patients and better interface with the leak-free trocars. In addition, the inside of each lumen was deburred with a Dremel tool to create a smooth finish on the inside of the lumens. This allowed for better integration of the electronic devices and helped to clear out any debris left inside either lumen. The wall thickness

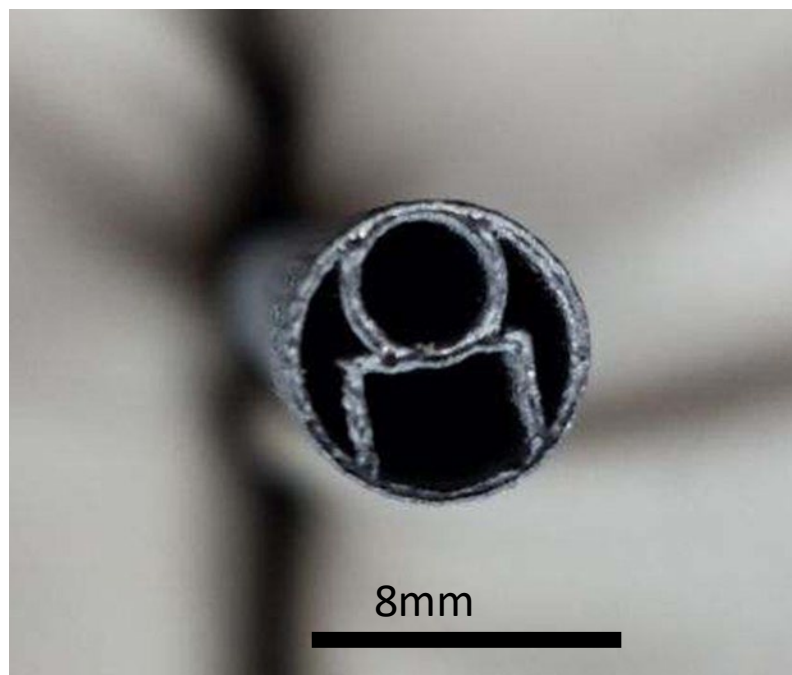


Figure 29: End-view of the Design VI shaft without any electronics implemented

was created to be 0.015 mm at all parts. The outside diameter of the shaft was 8mm in order to be compatible with commercially available trocars and remain a size that was clinically relevant.

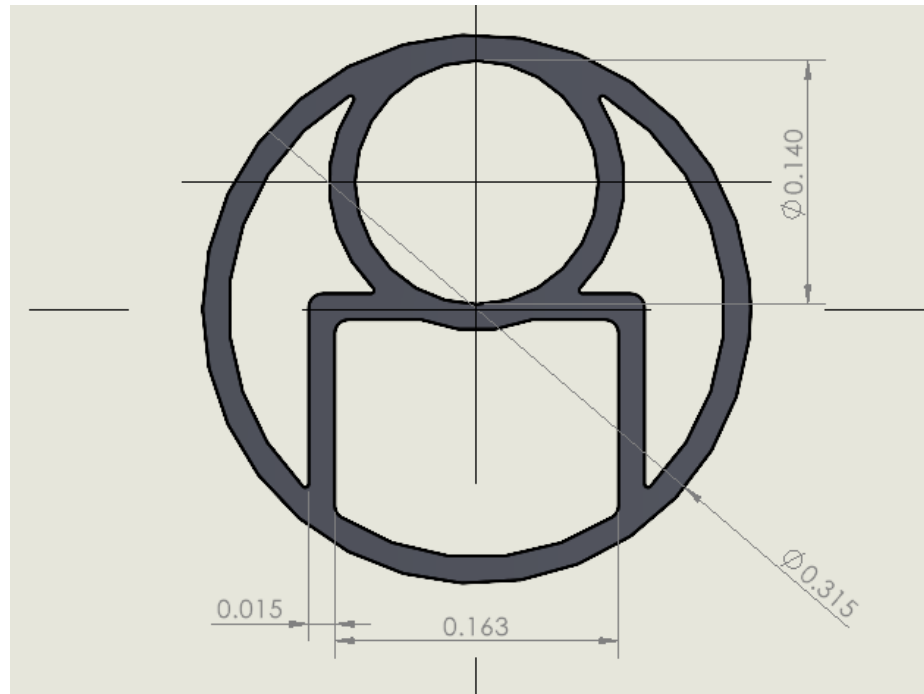


Figure 30: SolidWorks dimensioned model

3.2.9 Cautery Element

For the creation of the original cautery prototype, there was research that was completed to determine how to create and implement the prototype. It was decided that for Design VI thermal cautery would be used, where the creation of heat is from running a high current through a relatively low resistance circuit to apply power to heat up the surrounding tissue. The prototype from the Fall 2020 Capstone was used as a starting point for the cautery prototype for Design VI. This cautery prototype consisted of a piece of 14g copper wire approximately 2

inches long, wrapped in 2mm ID fiberglass tubing (uxcell brand) with about ½ an inch of the copper wire not inside of the fiberglass tubing, wrapped in nichrome wire (Master Wire Supply 28g), would be attached to a 12V battery to create heat (Figure 31). This was the original setup for the prototype to test that it would indeed create heat. This prototype was shown to work by attaching it to a battery to observed if heat was created. The measurement was taken via a Seek Thermal IR Smart Phone Adapter thermal camera (CompactXR, Model UT-AAA, Seek Thermal, Santa Barbara, CA) (Figure 32).

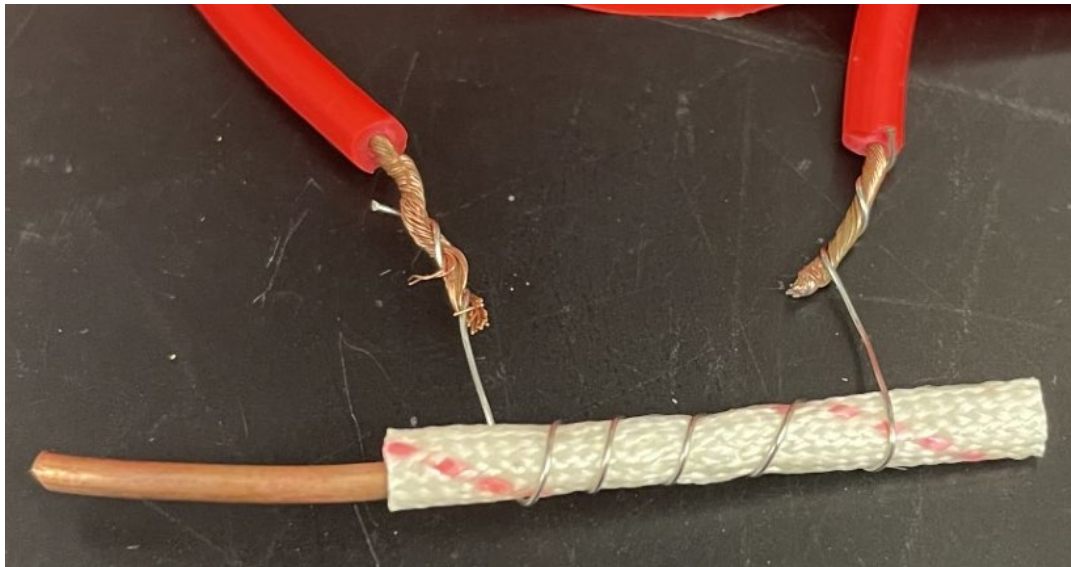


Figure 31: Unshielded cautery element prototype with electrically isolating fiberglass tubing between the copper and nichrome wire

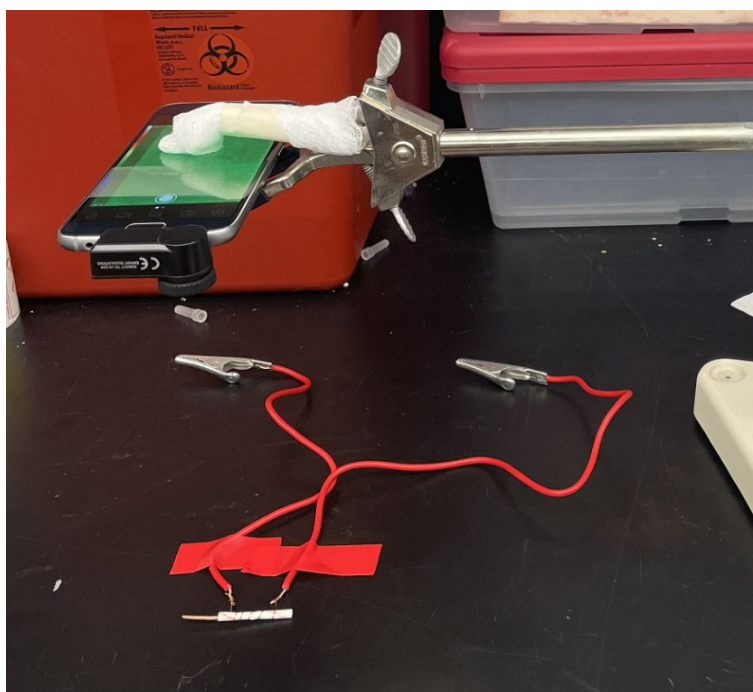


Figure 32: Setup using thermal camera for prototype development

A second prototype was created using high-temperature silicone heat shrink tubing instead of fiberglass tubing. This allowed the prototype diameter to be smaller and smoother, assisting in the integration into the designated lumen. The silicone isolated the copper rod electrically, which allowing heat to transfer to the copper (Figure 33). A second layer of heat shrink tubing was added around the nichrome coiling to separate the nichrome from the stainless-steel shaft. This second prototype was implemented into the MFSD shaft. This was glued in and sealed using high temperature silicone elastomer.

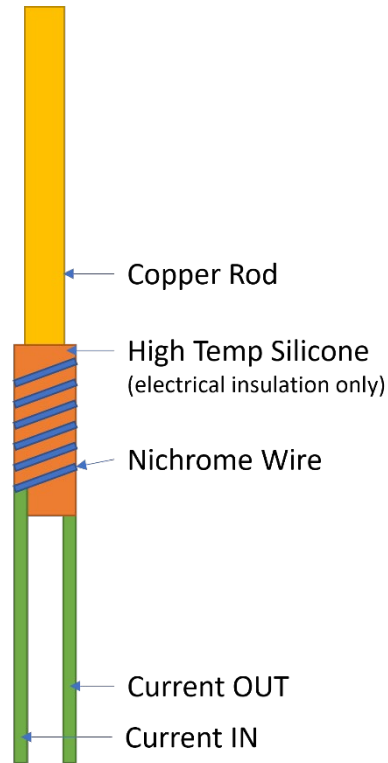


Figure 33: Schematic of the second cautery element (secondary outer silicone sheath not shown for clarity)

To modulate power to the heating element, a variable PWM signal was implemented. The Arduino PWM frequency is approximately 500 Hz and by adjusting the rate (in steps of 0-255 from off to on), the single 12V power supply could be used to create two different temperatures. By adjusting the PWM rate to limit the overall effective voltage, the two effective levels of cautery were applied. To accomplish this, the software was programmed to use two different pulse widths (90/255 and 120/255, or 35% and 71% of full-scale, respectively), and these frequencies were adjusted to reach the target temperatures for the dual temperature cautery. These modulation settings are what were used for benchtop testing and flight testing.

Current thermal devices can create power up to 36 watts like the SWH 014 Thermal Cautery device (Starwish Healthcare, New Delhi, India)

3.2.10 Clamshell Handle

The clamshell handle is what is held by the surgeon when using the device. The handle also houses electrical and fluidic components, including the button switch printed circuit board, the corresponding 3D printed pushbutton caps, the circuit board for the combined camera and LED light source, the silicone tubing attaching the suction and irrigation shaft, and all the wiring that goes back to the control system. This handle was 3D printed due to its unique shape. The design was printed in PLA (3D Solutek filament) using an Ender 6E FDM printer (Crealty.com, Shenzhen, China). This design was very similar to the previous design with the primary change being in how the shaft attaches to the handle. The inside clip attachments took away space from inside of the handle and were weak and often broke during printing, assembly, or use of the device. In order to claim space back inside the handle, and create a more secure attachment, the interface was moved to the end of the handle where a clip system was implemented to attach the shaft to the handle and to prevent it from spinning in the attachment.

3.3. Design V

The major difference between Design IV and Design V is the addition of the visualization function. The handle remained the same as the previous design. The same pushbutton caps and pushbutton circuit board was retained. The fluid path remained the same, and all electronics remained the same. The size of the

shaft stayed the same, however the internal lumens changed in size. The combined LED light and camera are larger than the fiberoptic LED in the previous design. This necessitated a redesign of the shaft, specifically the inner channels that create the multi-lumen shaft. This did create a smaller lumen for the suction and irrigation to flow through. The new shaft was designed in SolidWorks and was 3D printed by ProtoLabs in the same material, 316L Stainless Steel. The combined LED light and camera were taken from an Ambu disposable bronchoscope and filed down to reduced overall size in order to maximize the suction and irrigation lumen. The camera and LED light were glued into the end of the shaft, and the wiring was run down the handle. The circuit board for the LED light and camera was run out the end of the handle with the rest of the wiring. The circuit board was covered to protect it, but it was not placed in the control box. This design was assembled the same way: the pushbutton caps were placed in the handle, the pushbutton switch circuit board was placed in the buttons and screwed in, the shaft was clipped into the internal clips, the ¼" silicone tubing was attached to the shaft, and all electronic wiring and the silicone tubing was run out of the end of the handle. The 6-pin header for the button switch circuit board was attached to the control box, and the connector for the LED light and camera was plugged into the Ambu portable monitor to show the video and to power the LED light source. While this was an improvement over the previous design, the fifth function, cautery, was not yet implemented. In addition, the clips that held the shaft inside the handle were flimsy and kept breaking. These clips also took up a significant amount of space

inside the handle, and it was determined that the space inside the handle could be of better use housing electronics, like the printed circuit board that runs the combined LED light and camera. This would help to protect the circuit board, and the very thin wires that run between the camera and LED light, and the circuit board. This device was tested on two parabolic flights by completing a list of surgical tasks, and worked in tandem with the surgical immersion domes, and a manual fluid management system.

3.4. Design VI

The major difference between Design V and Design VI is the addition of the dual temperature cautery, the design of the shaft to incorporate the addition of the cautery function and the attachment between the shaft and the handle. Due to the addition of the cautery element, the size of the shaft was increased to 8mm, while all previous designs had a shaft diameter of 5mm. The 8mm shaft is still a clinically acceptable surgical instrument size. This new shaft has four lumens: one for the new cautery element, one for the new combined LED light and camera element, and two on each side to serve as the suction/irrigation lumens.

Due to the size of the light and camera, and the cautery element, they had to sit on top of each other, splitting the suction and irrigation into two lumens. However, this worked well as fail safe for clogs; if one side was clogged the other side could still complete the suction and irrigation task while clearing the other side. This shaft was printed in the same material, 316L Stainless Steel, however, this shaft was printed at AMIST at the University of Louisville. With the addition of

the cautery element, this required a creation of a prototype before incorporating it into the shaft.

The heating element did not change much from the original proof-of-concept in the Fall 2020 Capstone. The final heating element was a piece of thick copper wire but was changed to have heat shrink tubing as the intermediate material, instead of the fiberglass tubing material. The fiberglass material was burning, and would fall apart over time, allowing the heating element to no longer work. The heatshrink tubing, after being heated to melt and wrap around the copper wire, was then wrapped with the nichrome wire. Each of the coils were made tight to save in space and were wrapped without touching each other. Each end of the nichrome wire was soldered onto small gauge, insulated copper wire. The nichrome coils were then covered with shrink tubing. The copper wire was not put in the heat shrink tubing. Each of these layers allow heat to be transferred, but don't create a short circuit that would not allow the heat to be created. The insulated copper wires were fed down the lumen of the shaft, and the heating element was sealed as it was put into the shaft. Once sealed from the bottom of the element, it was then glued in place inside the shaft with temperature resistant glue. The end of the element was sealed on the top as well, allowing the tip of the heating element to remain exposed. Sealing on both ends prohibits the heating element from getting wet. The end of the lumen was sealed at the base of the shaft as a secondary precaution to prevent fluid from entering the electronics lumen of the shaft. Outside of the addition of the cautery element, and the subsequent design change in the shaft to accommodate said

cautery function, there also needed to be an improvement in the attachment between the shaft and the handle.

Previous designs incorporated internal clips inside the handle to attach to the shaft. However, these clips were flimsy and would often break either during assembly or use of the device. In addition, these clips and making the attachment internal to the handle took away some of the space inside the handle that could be better used for housing electronics. The internal clips were abandoned in favor of a peg and slot attachment style at the end of the device handle. The shaft had two semi-circles added to each side, which would serve as the pegs. The handle had two rectangles cut out near the tip of the wand, which would serve as the attachment slots. The shaft pegs would then be able to be placed inside the slots on the handle and would be held that way after the handle was attached together. The shaft would still attach to the silicone tubing but would be much higher in the device. Due to this, there was enough space inside the handle to incorporate the small circuit board for the combined LED light and camera, instead of having it external to the wand, in its own small case. This helped to protect the very thin wires from the LED light and camera, but also helped to further protect the circuit board from being damaged. All electrical cables still exited at the end of the device and would run back to the external control circuit. The handle was still attached with four self-tapping screws, and the same switch button circuit board, and 3D printed button caps were still used. This device was tested on two parabolic flight campaigns, and during the benchtop tests.

3.5. Tablet Controller for Flight Testing

For the parabolic flights that both designs V and VI were tested on, were accompanied by a tablet controller to run some of the external functions of the fluid control system, and display data. This software has a LabVIEW interface and is integrated with Arduino code programmed onto the microcontroller (Figure 34). This tablet displayed the acceleration, parabola count, time in zero gravity, a rolling list of the surgical activities to be completed, and several buttons and switches to run the pumps for the surgical immersion dome. There was a switch to change between filling the dome where all new water would be put into an empty dome, and purging the dome where new water would be put into an already full dome. There were two buttons to run the fill pump and the empty pump. Lastly, there was a switch to differentiate between venous and arterial simulated bleeding, with a button to run the small pump that would squirt in the simulated blood. The venous bleeding was when the pump would run at a slower, continuous speed creating an ooze of simulated blood, while arterial bleeding was when the pump would run at a faster oscillating speed creating pulsating

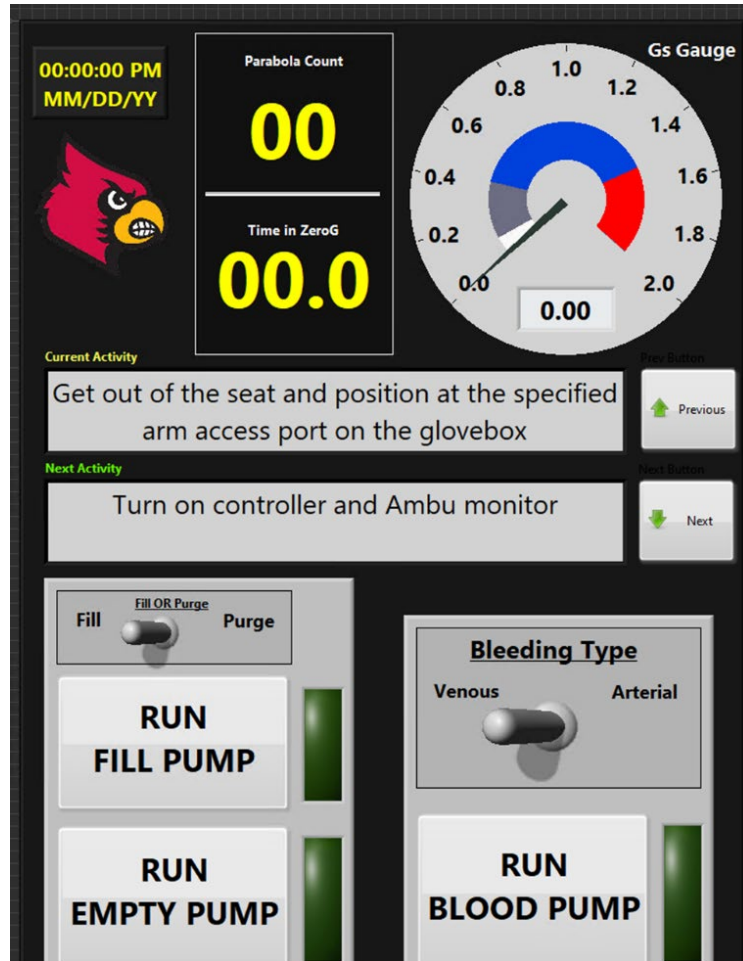


Figure 34: Screenshot of the tablet user interface for parabolic flight.

spurts of simulated blood. These changes were coded into the flight software to best replicate real bleeding patterns.

3.6. Portable Bronchoscope Monitor

Due to the fact that the combined LED and camera was taken from an Ambu Portable Bronchoscope, it was easiest to use the Ambu Portable Monitor for image display and capture since it was already compatible with the electronics cable from the LED light and camera. The end connector for the LED light and camera goes into the monitor to display the video and power the light.

For flight this monitor was attached to the wall of the Glovebox, powered by the internal battery and was used for the duration of the parabolic maneuvers.

3.7. Microcontroller

These designs were controlled by an 8-bit microcontroller (Arduino Nano, Figure 35). This device runs off a 5V operating voltage, contains 8 10-bit analog input pins and 6 PWM output pins. This board had a reduced footprint compared to the previous Arduino Uno, that was used in Design IV, with a similar operating power that allows for all five functions of the MFSD to be controlled and ran adequately.

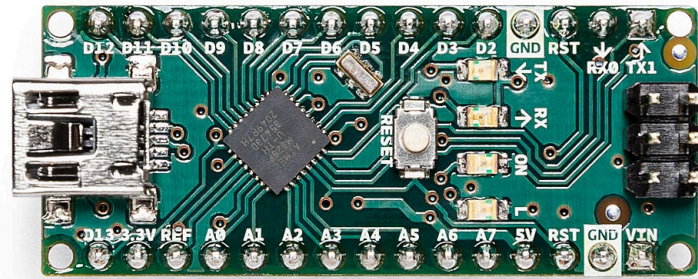


Figure 35: Arduino Nano

3.8. Flight Hardware

Both design V and VI were tested in two parabolic flights each. However, these are not stand-alone devices and require other equipment to complete these parabolic experiments. In addition to the device hardware outlined earlier, there are a few other miscellaneous pieces of equipment that are necessary to have in order to properly run and document these parabolic flights. A picture of the flight hardware ready for flight is shown in Figure 36. Two overhead cameras were used to get up close video of the surgical immersion dome and the second to get a complete view of the experiment board inside the Glovebox. The

cameras were Nikon KeyMission 170 and Sony HDR-CX 260V. In addition, the flight hardware included a commercially available endoscopic surgical device called the JustRight Pediatric Vessel Sealer. This device was used with the cord cut in order to act like a normal grasper. A custom holder was 3D printed for the MFSD to sit between flights and during in-flight transitions (Figure 37). A new leak-free trocar was also made to accommodate the new 8mm shaft size. This trocar was originally made from Delrin and copper tubing, but was later 3D printed for the November 2022 parabolic flights (Figure 38). Lastly, foam wound models were made to attach the surgical immersion dome to, and to house the tubing that the simulated bleeding comes from. Absorbent paper and gauze were also incorporated into the Glovebox to clean any unforeseen messes that may occur during flight.

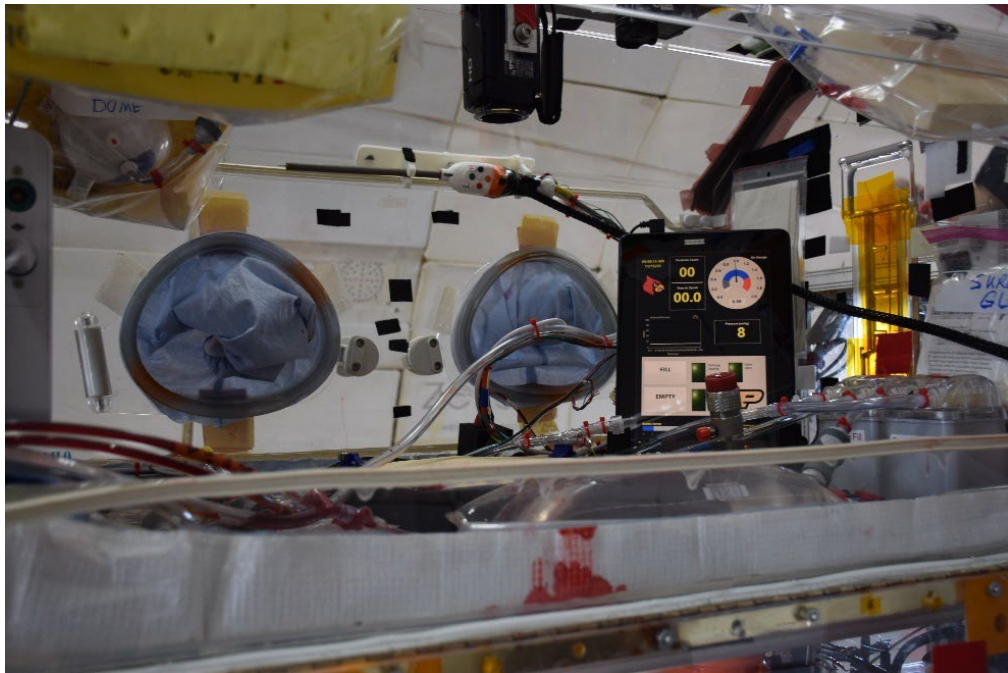


Figure 36: Side view of the flight hardware for parabolic flight.

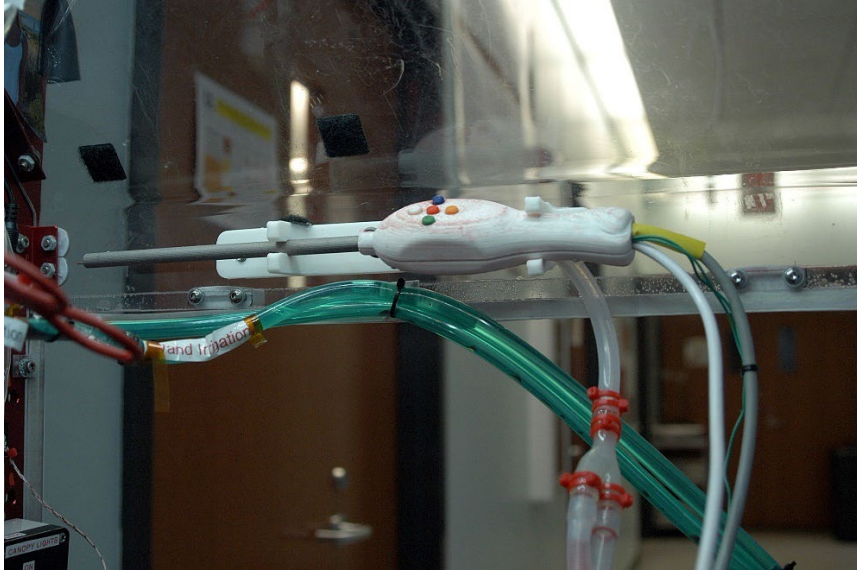


Figure 37: MFSD in its holder pre-flight.



Figure 38: Installed design development model of the final version of the 8mm leak-free trocar.

3.9. Control Software

In order to run the MFSD and its accompanying equipment, the use of a LabVIEW user interface was paired with code running on an Arduino to execute the functions of the experiment. This software would constantly monitor button presses from the wand and on the tablet interface. In addition, it constantly read the acceleration of the incorporated accelerometer in the printed circuit board to count parabolas, time in zero gravity and relay real-time acceleration data. This software also ran the filling, purging, and emptying of the dome, in addition to the operation of the simulated bleeding. Lastly, the software worked to read the button presses from the MFSD to work both temperatures of cautery, and to run the suction and irrigation for the MFSD through the shaft of the device. A full copy of the Arduino code, and screenshots of the LabVIEW code are shown in Appendix A and B.

3.10. Verification and Validation

3.10.1. Leak Testing

For the MFSD design, the leak testing was conducted through each step of assembly to ensure that no liquid would escape the interface between the shaft and the silicone tubing, including the portal hole where the electronics wiring exits the silicone tubing. After the silicone tubing was attached, and the portal hole was sealed with marine silicone elastomer the interface was tested by attaching it to the irrigation pump and running water through the shaft. The interface between the shaft and the silicone tubing, as well as the portal hole was observed as the water was run through for any leaks that may occur.

3.10.2. Suction and Irrigation Testing

Since the pumps between the previous design IV did not change into designs V and VI, it was deemed unnecessary to re-test the flow rate. The suction and irrigation testing for design VI had the goal of qualifying the effectiveness of the new double lumen suction and irrigation. Although the overall area of the suction and irrigation lumen was larger, the lumen was split into two lumens on either side of the cautery, light and camera elements. In order to qualify the suction and irrigation effectiveness, during the benchtop and the in-flight tests the irrigation was used to irrigate the simulated wound, and the suction was used to suction the simulated bleeding. Suction could also be used to empty the dome at the completion of the surgical tasks. Additional observations included if the lumens ever got clogged, and how the device would react in the case it did become clogged. Each time, observations were made by both the surgeon and a second investigator further referred to as “cap com”. The cap com recorded all observations on clipboard during flight and were referred to later in the post-flight debriefs. The suction was tested on both the simulated arterial and venous bleeding due to the varying flow rates and characteristics of the simulated bleeding.

3.10.3. Illumination and Visualization Testing

For the verification of the illumination and visualization testing, and qualitative analysis was done to ensure the illumination and visualization were adequate and at the same level of quality as the portable bronchoscope itself. Both the Ambu portable bronchoscope and the MFSD were tested in the same

manner. Whichever device being tested would be plugged into the portable bronchoscope monitor. This would allow the camera and light to be powered. The camera would then be pointed at a few pre-determined objects: the countertop, a piece of textured foam, and the pad of a finger. Screenshots were taken for each object, using each device. These photos were then compared. Each photo was judged for its clarity, brightness, and sharpness of the image, and each comparable image for each device was compared. Similar tests were conducted with the bleeding wound model during simulated bleeding and with the surgical instrument being manipulated.

3.10.4. Cautery Testing

When testing the cautery function one quantitative and one qualitative test was conducted.

The quantitative test utilized a Seek Thermal IR Smart Phone Adapter thermal camera (CompactXR, Model UT-AAA, Seek Thermal, Santa Barbara, CA). This thermal camera has a measuring temperature range of -40°C to 330°C, a reported thermal sensitivity of 0.07° C, and a frame rate of <9 Hz. Accuracy, however, was not reported so all temperature measurements were assumed to be within a few degrees of the reported values. This thermal camera plugged into an Android phone (Samsung) and measured the temperature of the cautery element during use and provided a video capture and static images of the temperature range. Both the low temperature and the high temperature cautery settings were enabled, and a video was taken of the temperature gradient. Both the amount of time it took to get to maximum temperature and the maximum

temperature was recorded. These measurements were performed three times for each temperature to ensure accuracy and repeatability in the temperatures created by the MFSD.

Finally, a qualitative use test was completed by using it on a source of biological tissue to see how it worked in an application setting. This was completed during the parabolic flights using tissue from scallops. These scallops were purchased the day before from the local supermarket. They were fresh mini scallops kept on ice between the tests. Each scallop was tested whole and was not patted dry before use. The scallop was attached to the simulated wound model and during flight both the low and high temperature cautery was used on the scallop and observations were made by both the investigator and the cap com.

3.10.5. Stand-Alone Control Testing

Before each flight test, each MFSD function was verified. Once the device was assembled and attached to the external control box, each function was activated to ensure it was ready for flight testing (Figure 39). The suction and irrigation functions were run for a few seconds to ensure there were no clogs in the shaft, that both the suction and irrigation pump would turn on with the corresponding button presses, and that both the suction and irrigation physical buttons were not stuck or obstructed during assembly. The illumination and visualization functions were verified by plugging in the external cord to the portable Bronchoscope monitor. The picture quality and brightness of illumination would then be observed to ensure the camera quality was still adequate to

complete the surgical tasks with, and that the light or camera was not obstructed during assembly. Lastly, the cautery functions were verified by turning both buttons on and measuring the temperature using the Seek Thermal Camera. This

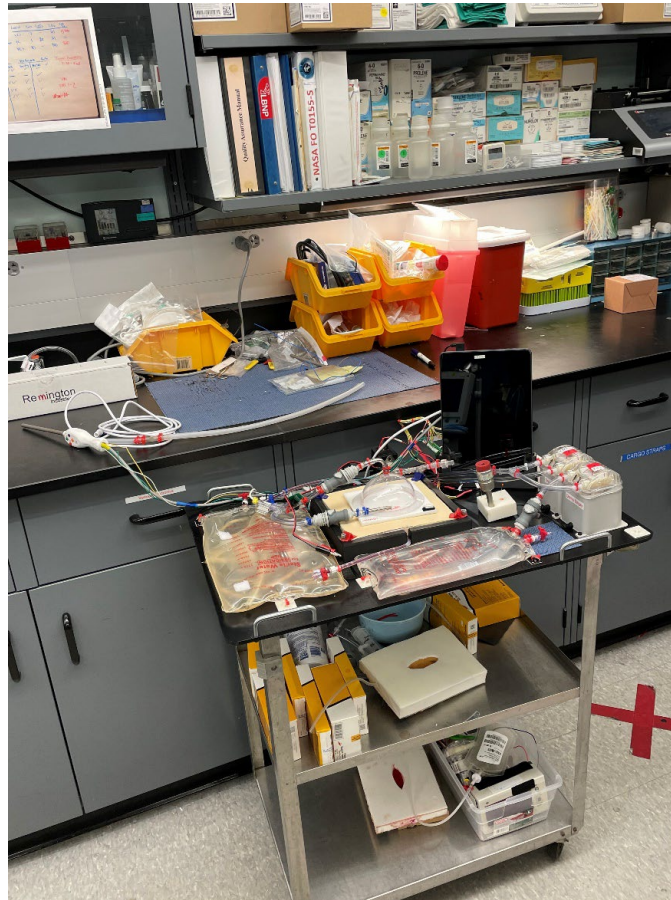


Figure 39: Experimental layout for the stand-alone testing for the MFSD before flight.

final step was performed to ensure that the element would still create heat, no wires were disconnected during assembly, and that the corresponding cautery buttons were not stuck or obstructed during assembly. Once each of the five functions were verified to work, the wand was then carefully packed to be transported for the flight campaigns.

3.11. Flight Testing

Since the application of this device is for use in zero gravity, the fully functional device was tested in a series of parabolic flights. These flights are accomplished using the company Zero-G. This company completes parabolic research flights where the plane will fall at the same rate as the equipment and investigators in order to simulate reduced and zero gravity. This is completed by flying in a set of parabolas where there are portions of reduced gravity during the falling, and hyper gravity during the pull up of the plane. These flights consist of six sets of five parabolas where each reduced gravity section lasts between eight and fifteen seconds. During each flight, the MFSD was integrated into a manually operated fluid management system. The MFSD would be used in tandem with an endoscopic grasper to complete surgical tasks simulating what it would be like to



Figure 40: Overhead view of the flight hardware with the MFSD being used inside the surgical containment dome attached to a bleeding wound model

complete a surgery in zero gravity (Figure 40). The MFSD was used both inside and outside the surgical immersion dome using the leak-free trocars as the interface. All five functions were utilized during flight and observations were recorded by the surgeon and the cap com. First all five functions were verified by testing both the suction and irrigation, ensuring the LED light was powered on, the camera was showing clear video, and that both temperatures of cautery were functional using the scallop tissue sample. Once all the functions were confirmed functional, the experimental surgical tasks were completed using a script that was created pre-flight to assist the user to follow the pre-planned sequence of steps. In addition, these tasks were recorded using two different overhead cameras inside the Glovebox. These videos were referenced during the flight debriefs and all observations were recorded in order to improve upon in the next flight campaigns and future MFSD designs. Figure 41 shows the layout for flight before being installed in the aircraft.

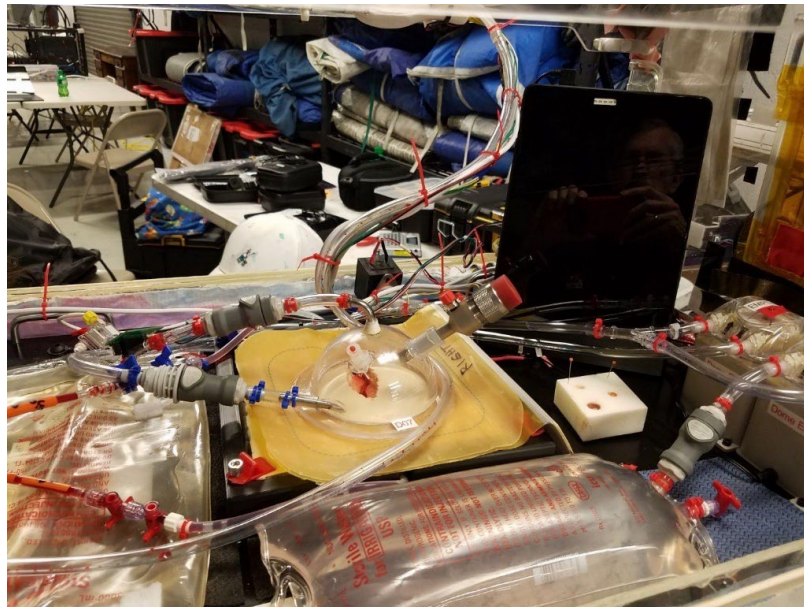


Figure 41: Side view of the flight layout that was used to test Design VI.

IV. RESULTS

4.1. Illumination and Visualization Integration

The combined LED light and camera was installed inside its custom lumen and sealed from both sides after insertion. The camera PCB was installed carefully into the inside of the wand handle. Once the combined LED light and camera was integrated into the shaft and the circuit board was reconnected, the functionality of the device was verified by plugging it into the portable Ambu monitor to ensure that the video showed, and the light turned on.

For Design V, when the camera was initially installed into the shaft, the video indicated that the camera was installed upside down (Figure 42). Since the shape of the combined LED light and camera were more of a trapezoid shape, it could only fit in the lumen facing one direction causing the image to show inverted. For this design, the camera was left inverted, since the monitor could be turned over for the time being. However, note was taken of this and was fixed for Design VI. Besides this, images were captured indicating that the illumination and integration were successful. In addition, this design did not house the printed circuit board in the handle of the device. Due to how the shaft attached to the inside of the handle, it took up too much internal space and the printed circuit board did not have enough room to fit inside the handle of the MFSD. A second 3D printed box was added around the circuit board and was left external to the

handle (Figure 43). This created issues since the wire is so thin it would routinely break and need to be reattached. In addition, the extra box hanging from the device prohibited some movement of the MFSD during used. Both of these issues were taken note of and were able to be fixed in the next design. Once the camera was properly installed and sealed, the wires from the combined LED light and camera were poked out of the silicone tubing into the handle. Once the wiring was reattached to the printed circuit board and the functionality of this element was confirmed, the exit portal in the silicone tubing was sealed with marine epoxy to prevent movement and the leaking of water.

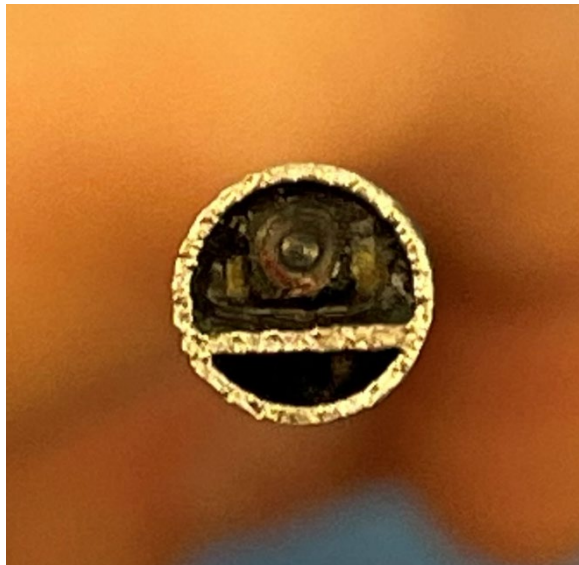


Figure 42: Tip of the Design V shaft with the combined LED light and camera installed

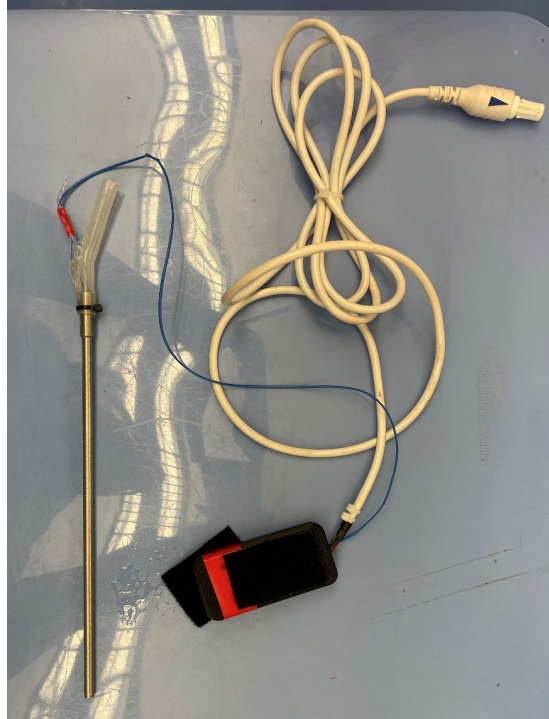


Figure 43: External cord and the 3D printed enclosure to isolate the camera electronics.

For Design VI, the combined LED light and camera was able to be sanded down further to create closer to a rectangle shape as opposed to the previous trapezoid shape. This allowed for it to fit easily in the designated lumen of the shaft (Figure 44). The connecting wires were fed down through the lumen of the shaft and into the handle to be reattached to the printed circuit board now housed in the handle. Both ends of the camera were sealed into the lumen, and a third seal was created at the end of the shaft that attaches to the MFSD. The same method was used above to finish the implementation of the combined LED light and camera. Once the camera was properly installed and sealed, the wires from the combined LED light and camera were passed through the silicone tubing into the handle. Once the wiring was reattached to the printed circuit board and the

functionality of this element was confirmed, the exit portal in the silicone tubing was sealed with marine epoxy to prevent movement and the leaking of water. Since Design VI adjusted the method of attachment between the shaft and the handle of the MFSD, there was now plenty of space inside the handle for the LED light and camera printed circuit board to be attached. The circuit board was glued to the inside of the handle, on the opposite piece to the button printed circuit board. The back of the button printed circuit board and the top of the LED light and camera printed circuit board were covered with hot glue to prevent breakage and from the electronics touching. This design had a fully functional LED light and camera, the printed circuit board was implemented into the handle and the camera was facing the correct way for the monitor to be properly used.



Figure 44: Combined LED light and camera implemented into the shaft of Design VI

4.2. Suction and Irrigation Wand

The suction and irrigation shaft was manufactured at AMIST at the University of Louisville (Figure 45). The shaft was 3D printed by direct metal laser sintering in 316L Stainless Steel. This material was chosen to make the shaft of the MFSD durable, resistant to corrosion and biocompatible. The shaft was sand blasted after manufacturing, and the insides were smoothed with a Dremel tool in order to make a smooth internal surface to assist with function integration.



Figure 45: Side view of the Design VI MFSD shaft

4.3. Cautery Element

This element was only implemented into Design VI. Design V had the primary purpose of implementing the LED light and camera, meaning this Design was not designed with a lumen to accommodate the cautery element. The primary hurdle with the cautery element in Design VI was the small size lumen it had to fit into. The design of the cautery element was still very similar to the prototype created during the 2020 Fall Capstone project, but the execution and the materials chosen were improved (Figure 46). While the copper wire, high temperature silicone shrink tubing and nichrome wire would fit into the lumen with ease, there needed to be another layer between the heating element and the shaft of the MFSD to separate them both thermally and electrically. This added

extra size and created friction causing issues with implementation. Originally using the fiberglass fabric tubing for both layers was not thin enough to fit inside the lumen (Figure 47). Due to the diameter of the element and the friction of the fiberglass material, the fiberglass tubing was bunching up as it was being inserted into the lumen and prohibited the element from being fully inserted into the cautery lumen. In addition, it was likely that the bottom of the element was exposed since the fiberglass fabric was bunching causing it to pull up off of the heating element. This was not providing the thermal and electrical isolation needed. In addition, for the fiberglass tubing in between the copper and the nichrome wire, it would start to burn and degrade under the repeated heating. This would cause it to degrade and eventually created holes in the fiberglass tubing.

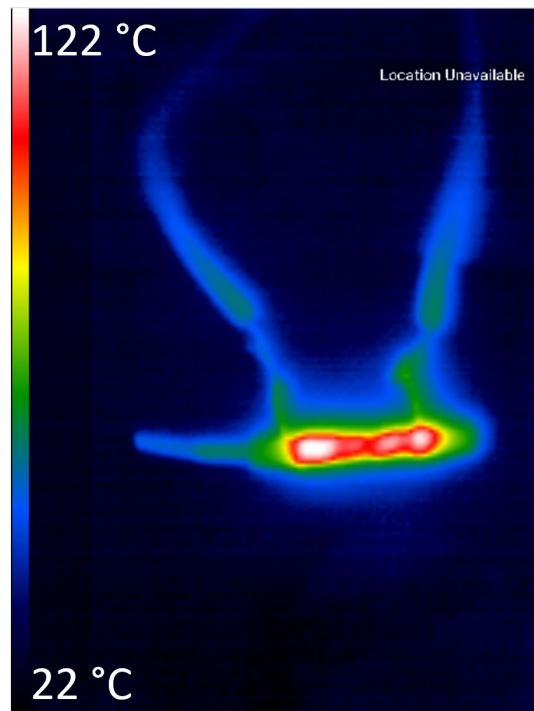


Figure 46: Showing the test of the original prototype that reached 122°C



Figure 47: Original cautery element in the fiberglass tubing intended to be implemented into the MFSD shaft

The fiberglass sheath material was not going to work as a long-term solution, so other materials were investigated. Silicone high temp heat shrink tubing was eventually used to electrically isolate the nichrome and copper wire and the heating element and the shaft. Since this material was smoother, was able to be heated to perfectly fit over the element which created an overall smaller element, this revision was able to be implemented. The long attachment wires were fed down through the shaft and out the end of the handle, and the element was sealed on both ends and on the end of the shaft that attached to the handle of the MFSD. After the attachment was made, the ending wires of the cautery element were attached to the control circuit, powered by the 12V power supply to ensure the connections survived the implementation, but also to assure

that the circuit was not shorted in anyway and still creates heat. After the connection, the buttons were pressed to ensure the two temperatures could be created still. Once the connection was deemed successful, the cautery wire extensions exiting the end of the shaft were poked out of the silicone tubing where the suction and irrigation fluid will travel, along with the wiring for the combined LED light and camera. Once the elements were properly installed and functionality was checked again, it was shown that the cautery function could be implemented into the MFSD and create the two-temperature cautery (Figure 48).

4.4. Clamshell Handle

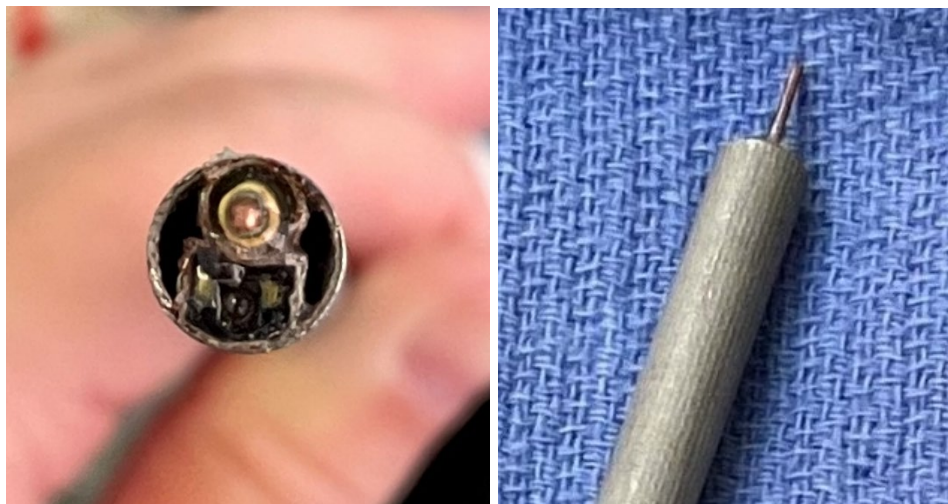


Figure 48: Tip of the new Design VI shaft. End view (left). Side view showing copper tip (right)

The primary difference between Design V and Design VI is the attachment between the shaft and the handle. The handle of Design V was the same as the previous designs, where the shaft attachment was a clip on the inside of the handle that attached to the end of the shaft, and then the shaft went out the front of the handle. The shaft attachment clips were weak and would often break

during assembly or use, and they took up a lot of space inside the handle that could be used for housing other electronics. Due to this, one of the large changes to Design VI was that the attachments for the shaft were moved to the tip of the handle. A set of semi-circles were added to the end of the shaft that would fit in two rectangular cutouts in the tip of the handle. This allowed the shaft to attach at the end of the handle and create more room inside the handle, which is now used to hold the printed circuit board for the combined LED light and camera. In addition, this new attachment was much stronger and did not break during assembly or use. Lastly, the hole at the end of the handle where the shaft attached was increased in size to accommodate the larger shaft diameter, since the shaft diameter increased from 5mm to 8mm. No other changes were made to the handle, it was still assembled the same way as usual, by using four self-tapping screws. The new attachments on the handle and the increase shaft diameter incorporated all of the wanted improvements and were able to function adequately and without failure.

4.5. Control Printed Circuit Board

The control printed circuit board was created to run all of the software functions of the wand, to read the buttons and to provide both input and output to the tablet controller. The control circuit board was tested on both the benchtop and during flight. In both instances, the printed circuit board fulfilled all its duties. The only issue was during the first parabolic flight for Design VI, the fuse for the cautery function blew and it needed to be replaced between flights with a higher amp fuse. All functions were able to be controlled by the circuit board and all of

the tablet buttons worked as designed. The accelerometer gave accurate acceleration feedback. It was shown to be effective and worked as designed.

4.6. Software

Both on the benchtop and during flight, the software was able to be debugged and adjusted to work in the optimal way for flight. The user interface was easy to use and intuitive that it required little or no instruction to outside users for them to be able to work it correctly. The back-end software provided all of the desired outputs to both the MFSD and its accompanying equipment.

4.7. Benchtop Testing

4.7.1 Leak Testing

During the initial leak testing, there was no leak observed in the connection between the shaft and the silicone tubing, but there was a small leak observed around the exit portal for the electrical wires. This was remedied by adding more marine epoxy where the water was leaking from. After allowing the epoxy to dry, the leak test was performed again, and there were no further leaks. As an extra precaution, the silicone tubing was zip tied onto the shaft, to ensure no water leaked with movement, and the silicon tubing did not get pulled off during use.

4.7.2 Suction and Irrigation Testing

During the suction and irrigation testing, both functions were tested, and observations were made. Both during the benchtop test and during the flight tests, the irrigation worked effectively at irrigating the wound and gave a steady

high rate of flow. For the suction testing, both arterial and venous bleeding were able to be suctioned quickly and without excess blood to pool. The suction was tested both with a full and empty dome and was able to suction adequately. In addition, the suction and irrigation lumens did not become clogged at any point, even with the clotting caused by the simulated blood. The updated dual lumen suction and irrigation system did not have any adverse effects and worked as well as the previous designs that only incorporated one lumen.

4.7.3 Illumination and Visualization Testing

For the illumination and visualization testing, it was deemed that the combined LED light and camera worked just as well as the Ambu bronchoscope camera before removal. All of the pictures taken were near identical and the clarity was adequate for use during the surgical tasks (Figure 49 & 50). The LED light was equally as bright on both devices being compared as well. The only difference was a slight yellow hue on the MFSD pictures. However, this was deemed not a large enough difference to affect the picture quality and the ease in completing the surgical tasks. Even with the removal of the extra potting material

around the LED light and camera, it worked just as well as the LED light and camera before removal.



Figure 49: Test photo from Design VI of the MFSD.

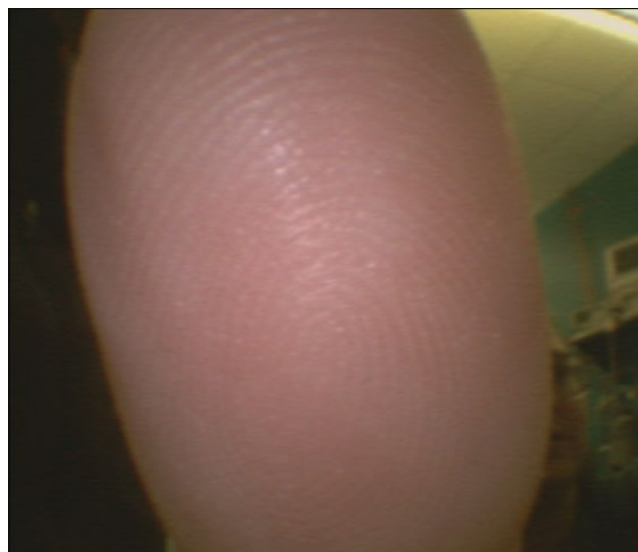


Figure 50: Test photo from the original Ambu bronchoscope.

4.7.4 Cautery Testing

For the quantitative portion of the cautery testing, we demonstrated that the MFSD cautery feature was able to create two different temperatures, and this was verified using the Seek Thermal Camera. The low temperature cautery setting created a measured maximum temperature of 85°C and took approximately five seconds to reach that temperature (Figure 51). The high temperature cautery setting created a maximum temperature of 104°C and took approximately eight seconds to reach that temperature (Figure 52). For the qualitative testing that was completed during flight, the MFSD was able to create a sizzle and burn mark on the tissue sample. Table 2 contains the temperature

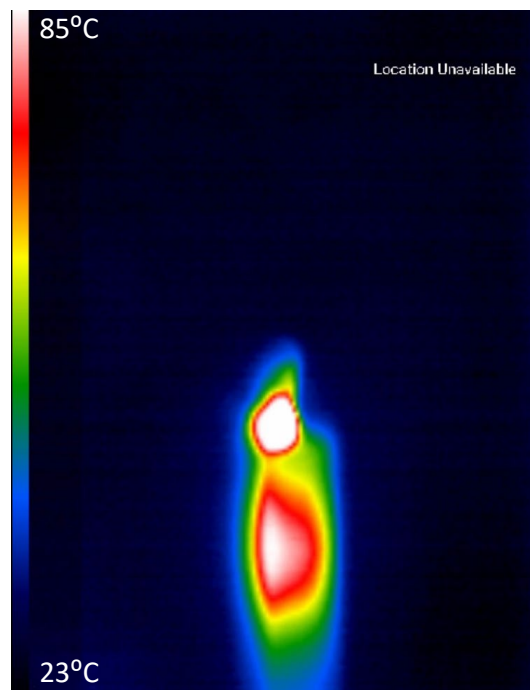


Figure 51: Maximum temperature observed was 85°C for the low temperature cautery.

values, Arduino PWM settings, and estimated power generated to create each temperature.

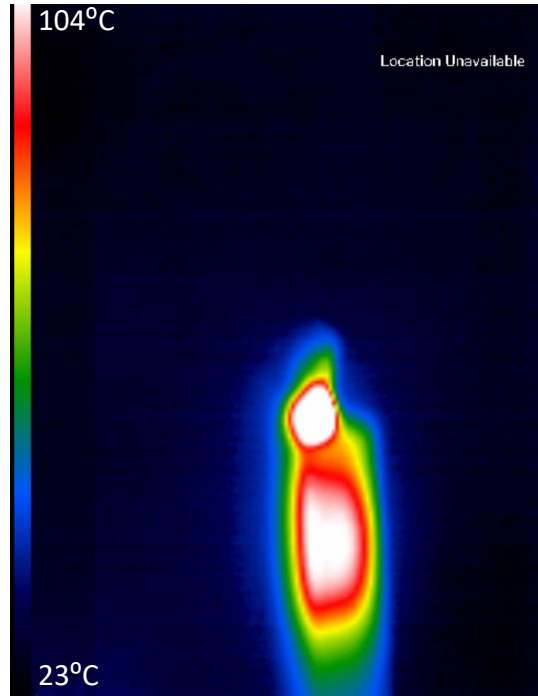


Figure 52: Maximum temperature observed was 104°C for the high temperature cautery.

Table 2: Cautery Test Results

| Control Setting | Arduino PWM | Duty Cycle Percentage | Measured Temperature (°C) | Estimated Power (Watts) |
|-----------------|-------------|-----------------------|---------------------------|-------------------------|
| Low | 90 | 35.3% | 85 | 1.79 |
| High | 120 | 47.1% | 104 | 3.19 |

4.7.5 Stand-Alone Control Testing

For the stand-alone control testing, all wand functions were deemed ready for flight. Each of them was in working order and activated with either the

appropriate physical button on the MFSD or the touch sensitive buttons on the tablet controller. This qualitative test was a simple check that everything was ready to be sent out for the parabolic flight campaigns (Figure 53).

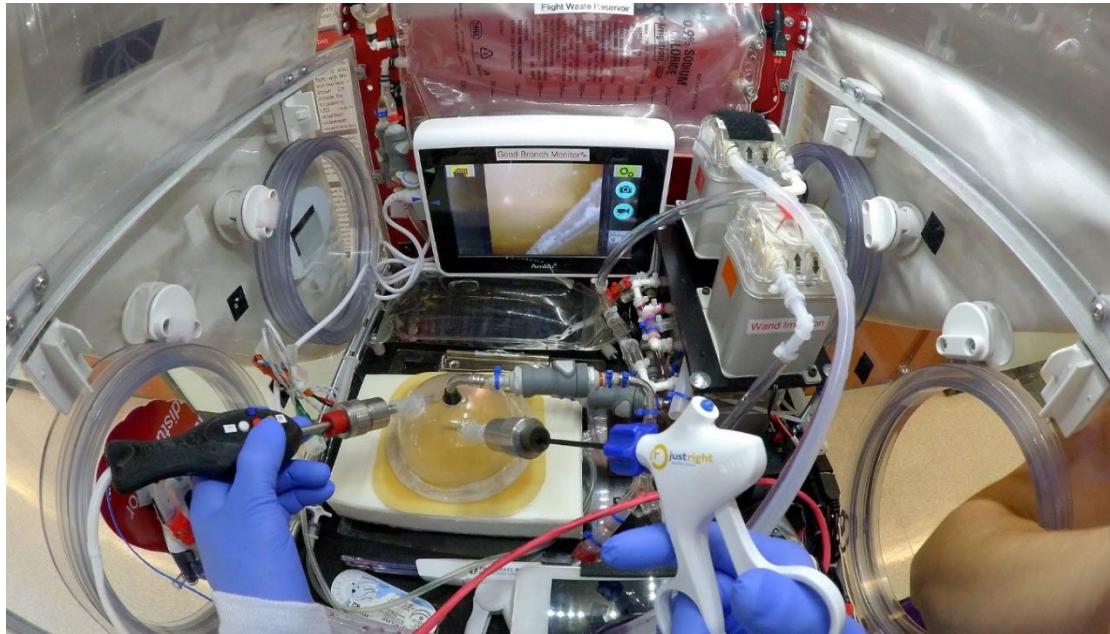


Figure 53: Image showing the pre-flight testing, including the functioning LED light and camera shown on the Ambu monitor.

4.8. In Flight Testing

For the final phase of MFSD testing, Design VI was tested over the course of four parabolic flight campaigns (30 parabolas each). The purpose of these flights was to test the MFSD and evaluate the needs for future suborbital flight testing of the entire system. With these flights, a script was created of common surgical procedures and what tasks needed to be completed in order to operate the other components of the system and test the MFSD. A singular investigator was using the Glovebox to test the functionality of the MFSD and complete the scripted tasks.

During the first of the four flight campaigns, the cautery function on the MFSD did not work. When either cautery button was pressed, no heat was created for either temperature setting, despite all other MFSD functions still operating properly. After inspecting the device post-flight, it was found that the fiberglass tubing on the inside of the MFSD shaft was degrading causing the nichrome wire to electrically contact the shaft resulting in the shaft heating up, instead of just the copper cautery tip. This failure was unable to be remedied by the second flight the next day, so the focus of validation of the system was temporarily shifted away from the cautery function to the other evaluations that were required. The combined LED light and camera worked well to both illuminate the area working and create a clear video of what was happening at the tip of the wand. The LED light powered on, and the video was shown on the Ambu monitor. All other surgical tasks were able to be completed, including irrigating the simulated wound, suctioning both simulated arterial and venous bleeding, and the other tasks not related to the MFSD. During the entirety of the first two flights, the MFSD did not leak internally or between the interface with the new 8mm trocar. The attachment between the shaft and the handle of the wand was a little bit loose for these flights but did not compromise the functionality of the MFSD.

All four surgeon investigators gave feedback on the MFSD, and overall, the notes were positive. It was of good size and shape to hold, was overall comfortable to use, easy to press the buttons, easy understand how it functioned,

and all of the functions worked to complete the simulated tasks, except the lack of cautery (Figure 54).

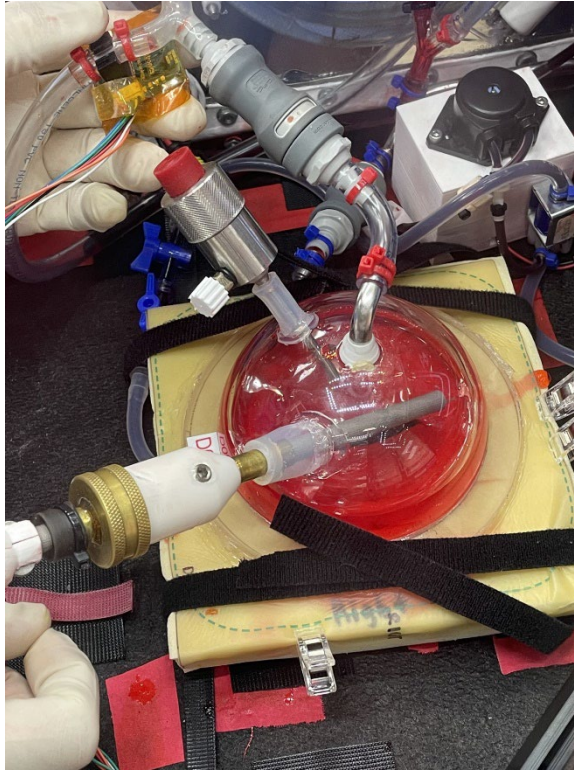


Figure 54: Partially filled immersion dome during experimental flight with the MFSD inserted via leak-free trocar.

For flights three and four, the cautery function did work and was able to be adequately tested during zero gravity. Between flights two and three, the old unshielded cautery element was removed and replaced. The new cautery element was able to be shielded with a silicone shrink tubing instead of the fiberglass tubing. This allowed the cautery element to be shielded between the copper tip and the nichrome wire, and the element was able to be shielded between the nichrome wire and the shaft of the MFSD. This allowed everything to be electrically separated, but still allowed the heat transfer to go from piece to piece to create the dual temperature cautery. During the third flight, although

enough heat was created to cause the sample to sizzle, the desired effects were not achieved by the low and high temperature cautery. Due to this, between flight three and four, the PWM threshold was increased to 90 and 120 on the low temperature and high temperature cautery, respectively, to create more heat with effectively higher applied voltages. There was some concern in how the circuit board and cautery function fuse would react to this increased power, but after some pre-flight testing, it seemed that the PCB mounted fuse would hold and work with the increased power. During the fourth flight, the same cautery test was run, and a significant burn was able to be created with the new increase in the power for the dual temperature cautery.

Overall, these flight campaigns were able to verify the efficacy of all five of the MFSD functions and that the additional characteristics needed to function in zero gravity were able to be met.

V. DISCUSSION

5.1. Design Review

There are a few sections of the design that can be reviewed individually for an overall evaluation of the device.

5.1.1 MFSD Shaft

Starting with the shaft of the MFSD, the 316L stainless steel worked well for the purpose of this device. This material is strong, easy to 3D print, resistant to corrosion, and biocompatible. This shaft was able to be ground down on the inside lumens to make the integration of the electronics easier. The design of this shaft was adequate to incorporate all of the functions set out to be implemented. It was a clinically relevant size at 8mm and could be used with commercially available trocars for endoscopic procedures.

5.1.2 MFSD Handle

The existing buttons in the MFSD handle were able to be used without modification, and overall, the handle was very similar to previous designs. The largest change was the mechanical attachment between the stainless-steel shaft and the handle. The new semicircle attachments add to the shaft design and the rectangles cut out in the handle worked as an alternative mounting technique that improved connection compared to the previous internal clips. This allowed for

more room inside the handle to hold other electronics and were more robust than the previous clips that would routinely break during assembly and use.

5.1.3 Functionality

With the functions of MFSD, each function was able to complete the task it was set out to do. While the dual temperature cautery was able to create adequate temperature, the functionality did not work as well as commercially available units when it comes to cutting and coagulation. However, it was still possible to observe the presence of coagulated tissue and a corresponding plume of steam from the site of cautery application.

As for the other characteristics of the MFSD needed to function in zero gravity, this wand was a completely sealed system that did not leak onto any of the electronics, including inside the handle. The suction and irrigation system operated as designed during use in zero gravity environment and did not clog during use in the flight campaigns.

5.1.4 Software and Electronics

Lastly, the software and complementary circuit board were updated to a state where users could work the MFSD with little to no instruction. Protocol feedback was provided via the tablet controller in the form of visual prompts for the user (Previous experiment step, Current experiment step, Next experiment step) and all functions were able to be tested with no issue.

5.2. Overall Summary

Overall, this final design was deemed a success as proof that a five function multi-functional device could be created with the application of space surgery in mind. This was shown through the benchtop testing and the multiple parabolic flights.

5.3. Limitations

The primary limitation for this project was budget restrictions. All precautions were taken to try to limit the amount of funds spent on this project, like fit testing the shaft and handle before having them printed in their final material. Ultimately that meant that larger ticket items, like having the final shaft 3D printed in the 316L stainless steel, were limiting on how many could be made. Overall, the total shaft fabrication costs were \$1072.50 over eight builds. Though only two were usable, each shaft cost about \$130 on average, and multiple test prints were required to get the design details and manufacturing process figured out.

In addition, there were some shortcomings of the equipment using to measure the cautery probe temperature. Most thermal cameras and other non-contact electronic temperature measuring devices are expensive, the Seek Thermal Camera was borrowed and used to measure prototype temperature. These bolometer-based devices have a tolerance related to temperature accuracy (reported Temperature $\pm X$ °C/F). The Seek device tolerance was not reported, so the temperatures measured are estimated to be within +/- 5 degrees

which is a conservative device since other devices are typically reported as Temp ± 2 to 3 degrees.

5.4. Future Work

Although the final Design VI was a huge improvement on the previous designs, there were still a few small improvements to be made, and other elements that could be incorporated to help the device function better and with more capabilities.

5.4.1 Wand Handle

The first improvement would be to modify the geometry of the semicircle and slot attachment between the shaft and the handle of the device. Although it fit in Design VI, it was slightly loose at the attachment location. This was remedied by putting a zip tie in between the shaft and the handle attachment, but this is not a permanent solution. A better fit for these attachments could be modified and a new handle could be printed. To stay within the current accepted sizes for endoscopic equipment, the overall diameter of the shaft cannot change, i.e., there is more flexibility in modifying the handle. In addition, the handle is less expensive to print than the shaft.

5.4.2 Cautery Temperature Adjustment

The second improvement would be to add a section to the software and user interface to allow a user to adjust the two low/high cautery temperatures. Current surgical cautery controllers allow for the user to adjust the cautery power. Adding this to MFSD functionality would allow it to better emulate existing

surgical devices by allowing the output to be adjusted when necessary. Currently, the goal is to have the MFSD be able to function the same whether it is being used in a normal air environment, or whether it is being used inside the surgical immersion dome. Due to the immersion dome being filled with liquid at certain points to help clean the wound and apply pressure, this could cause some issues in the cautery element since it would have to give a higher temperature output for the same effect to be created when submersed in liquid. Adding the user modification control to modify cautery power would allow flexibility of use. Also, using a higher source voltage, perhaps 24V instead of 12V, would provide a high cautery power if necessary.

5.4.3 Cautery Element

A third improvement would be to improve the design of the cautery element. Although it was proven functional and applied enough power to create a small channel when the cautery tip was energized (cutting effect) and an obvious coagulation effect, the construction was tedious which made the design problematic. More development might streamline assembly steps and improve reliability. It seems that thermal cautery may not be as effective as electrocautery, so future work may be done to see if there is a safe and viable option to switch the cautery element from thermal cautery to electrocautery for better results.

VI. CONCLUSION

Overall, Designs V and VI of the MFSD were deemed both to be successful implementations of what was outlined in the project specific aims. Design VI was the first in the series of MFSD devices that incorporated all five functions that were originally outlined as the goal for this device. A double suction and irrigation lumen was implemented to increase the area of suction and irrigation. A combined LED light and camera was added into the device to save space in the shaft of the wand. Finally, a thermal cautery element was added to the Design VI to fulfill the goal of adding a dual temperature cautery function to the design. This design was tested along the way with benchtop testing and was tested in its full functionality in four parabolic flights. Although there are still some improvements that could be made, but for the first iteration of Design VI, this device is a promising step in the right direction that with some work could be once used millions of miles away during space flight.

REFERENCES

1. Moore, C., R. Svetlik, and A. Williams. *Designing for reliability and robustness in international space station exercise countermeasures systems*. in *2017 IEEE Aerospace Conference*. 2017. IEEE.
2. Imhof, B., et al., *How the design of a sleeping bag can support counter-measuring fatigue*. *Acta Astronautica*, 2013. **91**: p. 123-130.
3. Kostoglou, M. and T. Karapantsios, *COOKING IN SPACE: Current situation, needs and perspectives*. *Current Opinion in Food Science*, 2023: p. 101021.
4. Schmitt, H.H., *Return to the Moon*, in *Lunar Settlements*. 2010, CRC Press. p. 21-26.
5. Sherwood, B., *Principles for a practical Moon base*. *Acta Astronautica*, 2019. **160**: p. 116-124.
6. Smith, M., et al. *The artemis program: An overview of nasa's activities to return humans to the moon*. in *2020 IEEE Aerospace Conference*. 2020. IEEE.
7. Portree, D.S., *Humans to Mars: fifty years of mission planning, 1950-2000*. 2001: National Aeronautics and Space Administration.
8. Ehlmann, B.L., et al., *Humans to Mars: A feasibility and cost–benefit analysis*. *Acta astronautica*, 2005. **56**(9-12): p. 851-858.
9. Zubrin, R., *Case for mars*. 2011: Simon and Schuster.
10. Cichan, T., et al., *Mars base camp: an architecture for sending humans to Mars*. *New Space*, 2017. **5**(4): p. 203-218.
11. Nicogossian, A., *Medicine and Space Exploration*. *The Lancet*, 2003. **362**.
12. Grimm, D., *Microgravity and Space Medicine*. *International Journal of Molecular Sciences*, 2021. **22**(13).
13. Jones, J.A., et al., *Endoscopic Surgery and Telemedicine in Microgravity: Developing Contingency Procedures for Exploratory Class Spaceflight*. Elsevier Science, 1999. **53**(5): p. 892-897.
14. Pool, S. and J. Davis, *Space Medicine Roots: A Historical Perspective for the Current Direction*. *Aviat Space Environ Med*, 2007. **78**.
15. Nicogossian, A. and D. Pober, *The Future of Space Medicine*. *Acta Astronautica*, 2001. **49**(3-10): p. 529-535.
16. Rajput, S., *A Review of Space Surgery - What Have We Achieved, Current Challenges, and Future Prospects*. *Acta Astronautica*, 2021. **188**: p. 18-24.
17. Lee, Y., *Surgery in space*. *The Korean Journal of Aerospace and Environmental Medicine*, 2022. **32**(2): p. 39-43.

18. Covington, D.B. and R.E. Moon, *Anesthesia and surgery in space: Comment*. *Anesthesiology*, 2022. **136**(2): p. 399-399.
19. Pantalone, D., et al., *Robot-assisted surgery in space: pros and cons. A review from the surgeon's point of view*. *npj Microgravity*, 2021. **7**(1): p. 56.
20. Rajput, S., *A review of space surgery-What have we achieved, current challenges, and future prospects*. *Acta Astronautica*, 2021. **188**: p. 18-24.
21. Korte, C.M., *A preliminary investigation into using artificial neural networks to generate surgical trajectories to enable semi-autonomous surgery in space*. 2020, University of Cincinnati.
22. Bogomolov, V.V., et al., *International Space Station Medical Standards and Certification for Space Flight Participants*. *Aviation, Space, and Environmental Medicine*, 2007. **78**(12).
23. Panait, L., et al., *Measurement of Laparoscopic Skills in Microgravity Anticipates the Space Surgeon*. *The American Journal of Surgery*, 2004. **188**: p. 549-552.
24. Drudi, L., et al., *Surgery in Space: Where are we at now?* *Acta Astronaut*, 2012. **79**: p. 61-66.
25. Rafiq, A., et al., *Microgravity Effects on Fine Motor Skills: Tying Surgical Knots During Parabolic Flight*. *Aviation, Space, and Environmental Medicine*, 2006. **77**(8): p. 852-856.
26. Kirkpatrick, A.W., et al., *Severe Traumatic Injury during Long Duration Spaceflight: Light Years Beyond ATLS*. *Journal of Trauma Management & Outcomes*, 2009. **3**(4).
27. Martyn, Y., *Changes in Space Medicine Over the Last 50 Years*. *Occupational Medicine*, 2019. **69**: p. 314-315.
28. Hayden, J.A., et al., *A Hermetically Sealed, Fluid-Filled Surgical Enclosure for Microgravity*. *Aviation, Space, and Environmental Medicine*, 2013. **84**(12).
29. Surgeons, A.H.C.o.M.o.t.S.M.A.a.t.S.o.N.F., *Human Health and Performance for Long-Duration Spaceflight*. *Aviation, Space, and Environmental Medicine*, 2008. **79**(6).
30. Posner, E.C. and R. Stevens, *Deep space communication-Past, present, and future*. *IEEE Communications Magazine*, 1984. **22**: p. 8-21.
31. Opsomer, L., et al., *Dexterous manipulation during rhythmic arm movements in Mars, moon, and micro-gravity*. *Frontiers in Physiology*, 2018. **9**: p. 938.
32. *Cambridge Dictionary*. Cambridge University Press & Assessment.
33. *Electrocauterization*. Medline Plus.
34. Taheri, A., et al., *Electrosurgery: part I. Basics and principles*. *Journal of the American Academy of Dermatology*, 2014. **70**(4): p. 591. e1-591. e14.
35. Cordero, I., *Electrosurgical Units - How They Work and How to Use Them*. *Community Eye Health Journal*, 2015.
36. Covidien, *Principles of Electrosurgery*. 2008.
37. Pollock, S., et al., *Electrosurgery*. *Dermatology Mosby Elsevier*, 2008. **2**.

38. Frecker, M.I., et al., *Laparoscopic Multifunctional Instruments: Design and Testing of Initial Prototypes*. Journal of the Society of Laparoendoscopic Surgeons, 2005. **9**: p. 105-112.

VII. Appendix A: Arduino Test Code

```
#include <Ewma.h> // library available from https://github.com/VividCortex/ewma
Ewma adcFilterX(0.1); // Less smoothing - faster to detect changes, but more prone to noise
Ewma adcFilterY(0.1); // Less smoothing - faster to detect changes, but more prone to noise
Ewma adcFilterZ(0.1); // Less smoothing - faster to detect changes, but more prone to noise
Ewma adcFilterPress(0.1); // Less smoothing - faster to detect changes, but more prone to noise

float scale2Volts = 5.0/1024.0;
float scale2Gs = 1/0.330;

float scaleX = -0.0142;
float offsetX = 5.0249;

float scaleY = -0.0139;
float offsetY = 4.8952;

float scaleZ = -0.0142;
float offsetZ = 5.0721;

float scale2mmHg = -0.9645;
float offsetP = 510.32;

const int fillValve = 7;
const int threeWayValve = 8;
const int fillPump = 9;
const int emptyPump = 10;
const int cauteryWand = 11;
const int bloodPump = 12;
```

```

int bleedingState = 0; // can be 0 for venous or 1 for arterial
int isBleeding = 0;
int bloodPumpSpeed = 150; // speed in PWM of Blood Pump
int bloodPumpSpeedStep = 50; // how many points to increment the pump speed by (0-255)

// Wand handle inputs....
/*
Buttons:
  D2 suction white
  D3 left cautery blue
  D4 right cautery green
  D5 irrig orange
  D6 illum red
*/

const int suctionButton = 2;
const int cauteryLeftButton = 3;
const int cauteryRightButton = 4;
const int irrigateButton = 5;
const int illuminationButton = 6;

int irrigateState = 0;
int suctionState = 0;
int cauteryLeftState = 0;
int cauteryRightState = 0;

// the setup routine runs once when you press reset:
void setup() {
  // initialize serial communication at 9600 bits per second:
  Serial.begin(9600);

  pinMode(fillPump, OUTPUT);

```

```

pinMode(fillValve, OUTPUT);
pinMode(emptyPump, OUTPUT);

pinMode(threeWayValve, OUTPUT);
pinMode(bloodPump, OUTPUT);

pinMode(cauteryWand, OUTPUT);

pinMode(suctionButton, INPUT);
pinMode(cauteryLeftButton, INPUT);
pinMode(cauteryRightButton, INPUT);
pinMode(irrigateButton, INPUT);
pinMode(illuminationButton, INPUT);

digitalWrite(fillPump, LOW); // let's make sure this pump is off!!
digitalWrite(emptyPump, LOW); // let's make sure this pump is off!!

}

// the loop routine runs over and over again forever:

void loop() {

  // read the input on analog pin 0:
  int sensorValueX = analogRead(A3);
  float filteredX = adcFilterX.filter(sensorValueX);
  float sensorValueXScaled = scale2Volts * filteredX;
  // float XGs = sensorValueXScaled * scale2Gs * (-1.0) + offsetX;
  float XGs = filteredX * scaleX + offsetX;

  int sensorValueY = analogRead(A6);
  float filteredY = adcFilterY.filter(sensorValueY);
  float sensorValueYScaled = scale2Volts * filteredY;

```

```

// float YGs = sensorValueYScaled * scale2Gs - offsetY;
float YGs = filteredY * scaleY + offsetY;

int sensorValueZ = analogRead(A7);
float filteredZ = adcFilterZ.filter(sensorValueZ);
float sensorValueZScaled = scale2Volts * filteredZ;
// float ZGs = sensorValueZScaled * scale2Gs * (-1.0) + offsetZ;
float ZGs = filteredZ * scaleZ + offsetZ;

int bubbleSensor = analogRead(A0);
float bubbleSensorVolts = bubbleSensor * scale2Volts;

int pressureSensor = analogRead(A1);
float filteredPress = adcFilterPress.filter(pressureSensor);
float pressureSensorVolts = filteredPress * scale2Volts;
float pressuremmHg = filteredPress * scale2mmHg + offsetP;

// print out the value you read:
Serial.print(XGs);
Serial.print(",");
Serial.print(YGs);
Serial.print(",");
Serial.print(ZGs);
Serial.print(",");
Serial.print(bubbleSensorVolts);
Serial.print(",");
Serial.println(pressuremmHg);

/* Commands
0 - Fill Pump Off 48
1 - Fill Pump On 49
2 - Empty Pump Off 50

```

```
3 - Empty Pump On 51
4 - Bleeding State Venous 52
5 - Bleeding State Arterial 53
6 - Bleeding Off 54
7 - Bleeding On 55
8 - Cautery On 56
9 - Cautery Off 57
*/
```

```
while (Serial.available() > 0) {

    int commandInput = Serial.read();

    if (commandInput == 48) {
        // '48' corresponds to a '0' and will turn the Fill Pump OFF
        digitalWrite(fillPump, LOW);
        delay(25);
        digitalWrite(fillValve, LOW); // Close the valve AFTER turning off fill pump
    }
    else if (commandInput == 49) {
        // '49' corresponds to a '1' and will turn the Fill Pump ON
        if (irrigateState == 0) {
            // don't turn on if irrigation is on
            digitalWrite(fillValve, HIGH); // Open the valve BEFORE turning on fill pump
            delay(25);
            digitalWrite(fillPump, HIGH);
            delay(25);
        }
    }
    else if (commandInput == 50) {
        // '50' corresponds to a '2' and will turn the Empty Pump OFF
        digitalWrite(emptyPump, LOW);
    }
}
```

```

else if (commandInput == 51) {
    // '51' corresponds to a '3' and will turn the Empty Pump ON
    if (suctionState == 0) {
        // don't turn on if suction is on
        digitalWrite(emptyPump, HIGH);
    }
}
else if (commandInput == 52) {
    // '52' corresponds to a '4' and will set Bleeding State to Venous; Will NOT enable
    digitalWrite(threeWayValve, LOW);
    bleedingState = 0;
}
else if (commandInput == 53) {
    // '53' corresponds to a '5' and will set Bleeding State to Arterial; Will NOT enable
    digitalWrite(threeWayValve, HIGH);
    bleedingState = 1;
}
else if (commandInput == 54) {
    // '54' corresponds to a '6' and will set Bleeding State to OFF
    analogWrite(bloodPump, 0);
    isBleeding = false; // make sure that the state is NOT bleeding
    bloodPumpSpeed = 150;
}
else if (commandInput == 55) {
    // '55' corresponds to a '7' and will set Bleeding State to ON
    if (bleedingState == 0) {
        analogWrite(bloodPump, 255);
        delay(10);
        analogWrite(bloodPump, 190);
        delay(10);
        analogWrite(bloodPump, 128);
    }
    bloodPumpSpeed = 150; // start speed at zero
}

```

```

    isBleeding = 1;
  }
  else if (commandInput == 56) {
    // '56' corresponds to an '8' and will set Cautery State to ON at PWM 100
    analogWrite(cauteryWand, 100);
  }
  else if (commandInput == 57) {
    // '57' corresponds to a '9' and will set Cautery State to OFF
    analogWrite(cauteryWand, 0);
  }
  else {
    Serial.println(commandInput); // hiccup the output to show some error
    delay(1000);
  }
}
// end of serial while

// The Below controls the speeding up and slowing down of the blood pump... only if bleeding
state is 0

if (isBleeding == 1 && bleedingState == 1) {
  analogWrite(bloodPump, bloodPumpSpeed); // set the blood pump speed
  bloodPumpSpeed = bloodPumpSpeed + bloodPumpSpeedStep; // change the speed for the
next time through the loop
}

if (bloodPumpSpeed <= 0) {

  bloodPumpSpeedStep = -bloodPumpSpeedStep;
}

if (bloodPumpSpeed >= 255) {
  delay(500);
  bloodPumpSpeedStep = -bloodPumpSpeedStep;
}

```

```

    }

    if (digitalRead(irrigateButton) == HIGH) {
        digitalWrite(fillPump, HIGH);
        irrigateState = 1;
    }

    if (irrigateState == 1 && digitalRead(irrigateButton) == LOW) {
        irrigateState = 0;
        digitalWrite(fillPump, LOW);
    }

    if (digitalRead(suctionButton) == HIGH) {
        digitalWrite(emptyPump, HIGH);
        suctionState = 1;
        delay(25);
    }

    if (suctionState == 1 && digitalRead(suctionButton) == LOW) {
        suctionState = 0;
        digitalWrite(emptyPump, LOW);
    }

    if (digitalRead(cauteryLeftButton) == HIGH) {
        analogWrite(cauteryWand, 35);
        cauteryLeftState = 1;
    }

    if (cauteryLeftState == 1 && digitalRead(cauteryLeftButton) == LOW) {
        cauteryLeftState = 0;
        analogWrite(cauteryWand, 0);
    }

```

```
if (digitalRead(cauteryRightButton) == HIGH) {  
    analogWrite(cauteryWand, 90);  
    cauteryRightState = 1;  
}  
  
if (cauteryRightState == 1 && digitalRead(cauteryRightButton) == LOW) {  
    cauteryRightState = 0;  
    analogWrite(cauteryWand, 0);  
}  
  
delay(10);    // delay in between reads for stability - this delay is approximately 100 Hz  
}
```

VIII. Appendix A: LabVIEW Test Code

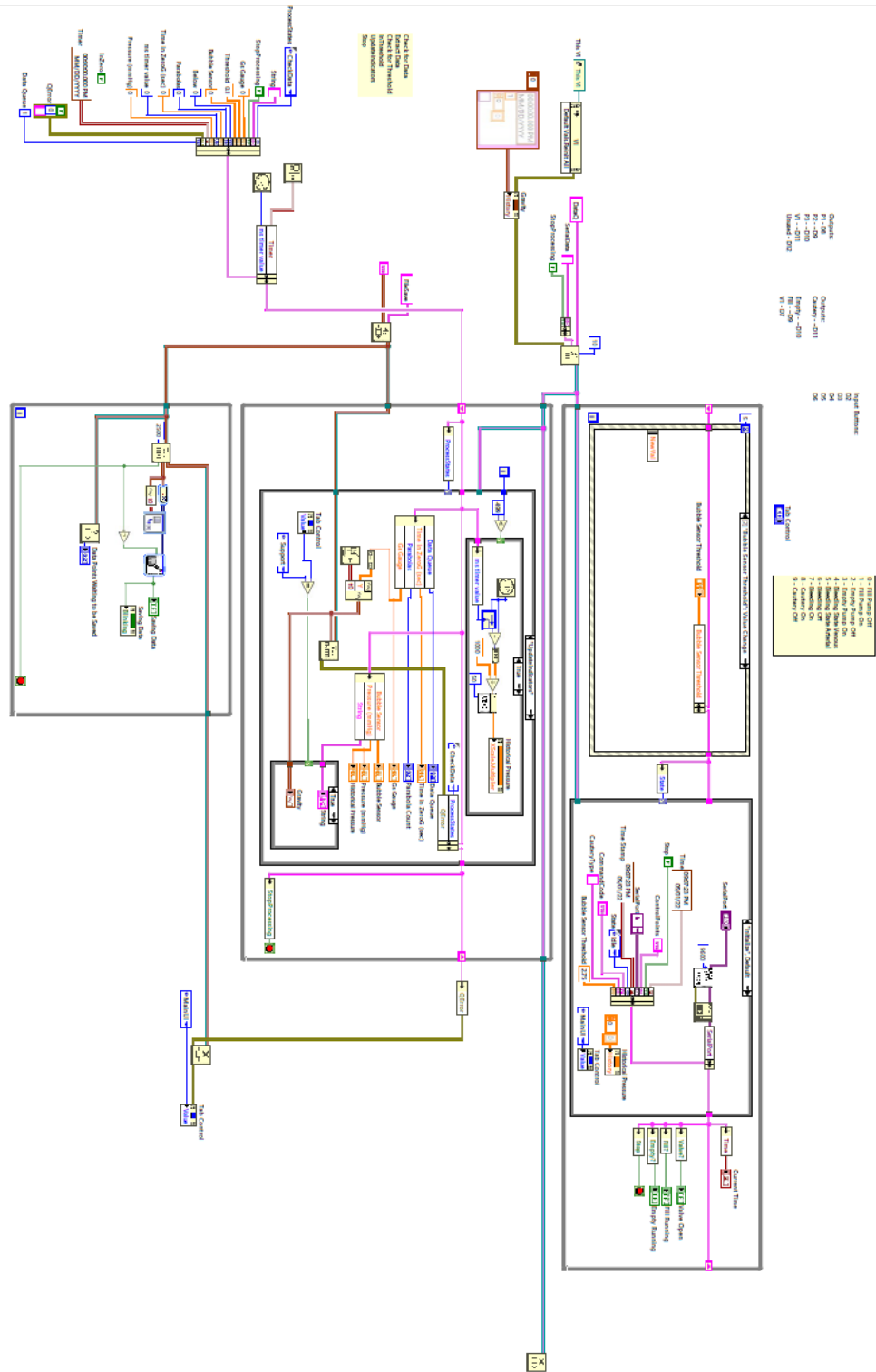


Figure 55: Full Block Diagram of LabVIEW code

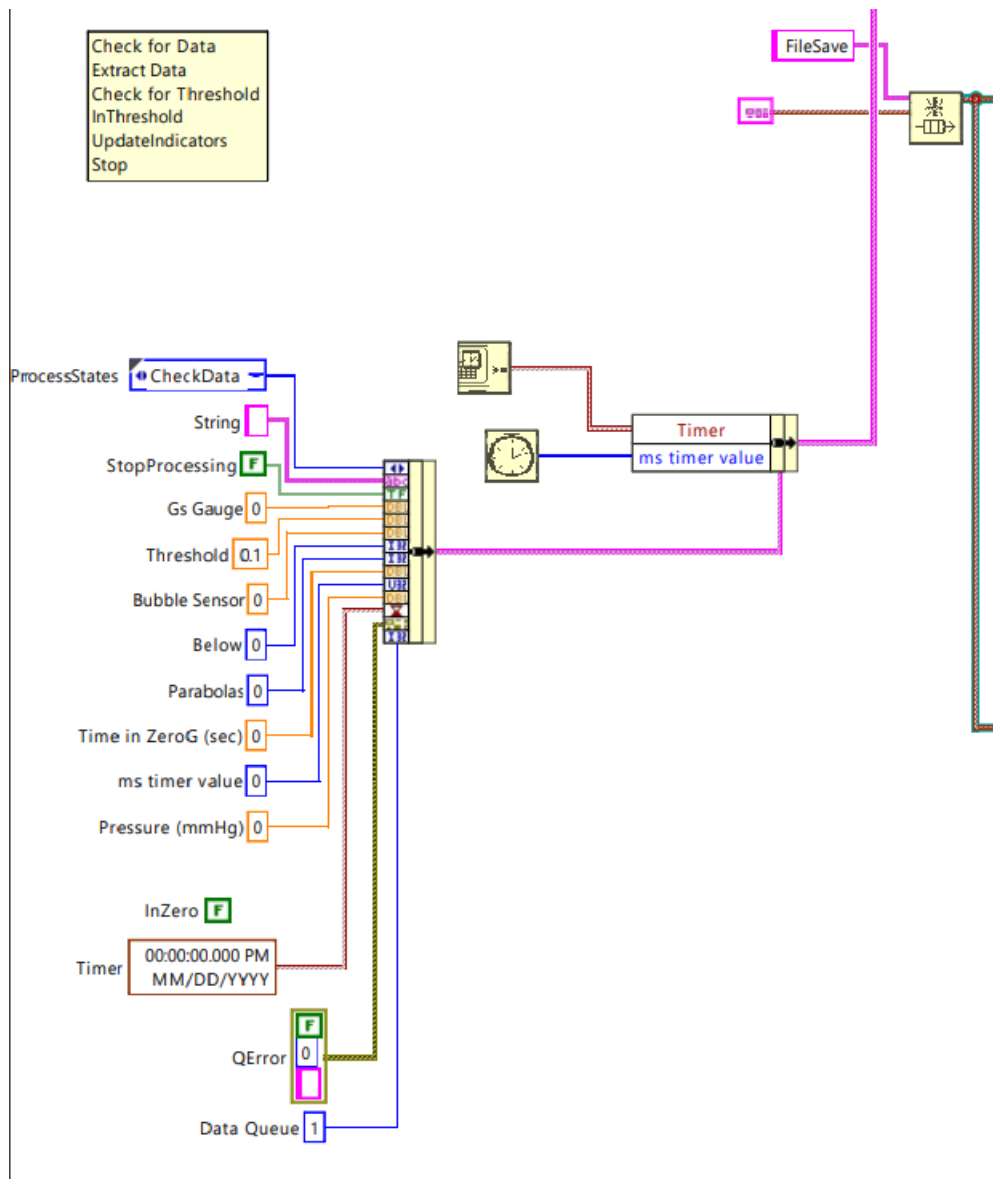


Figure 56: Closeup of Master Cluster showing system variables

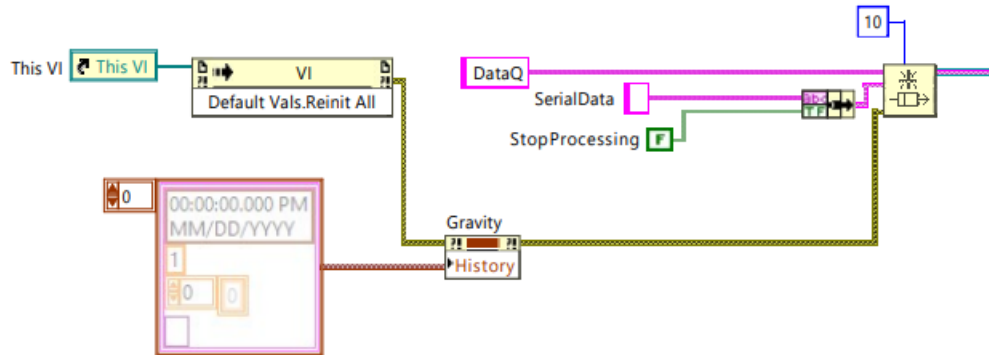


Figure 57: Close up of Data Queue creation

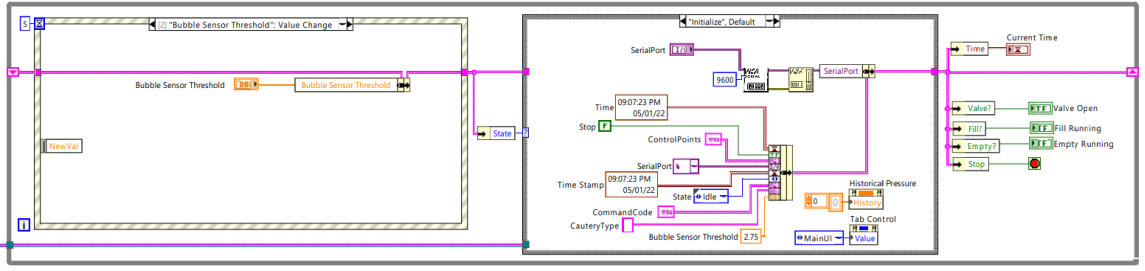


Figure 58: Close up of User Event Structure and State Machine

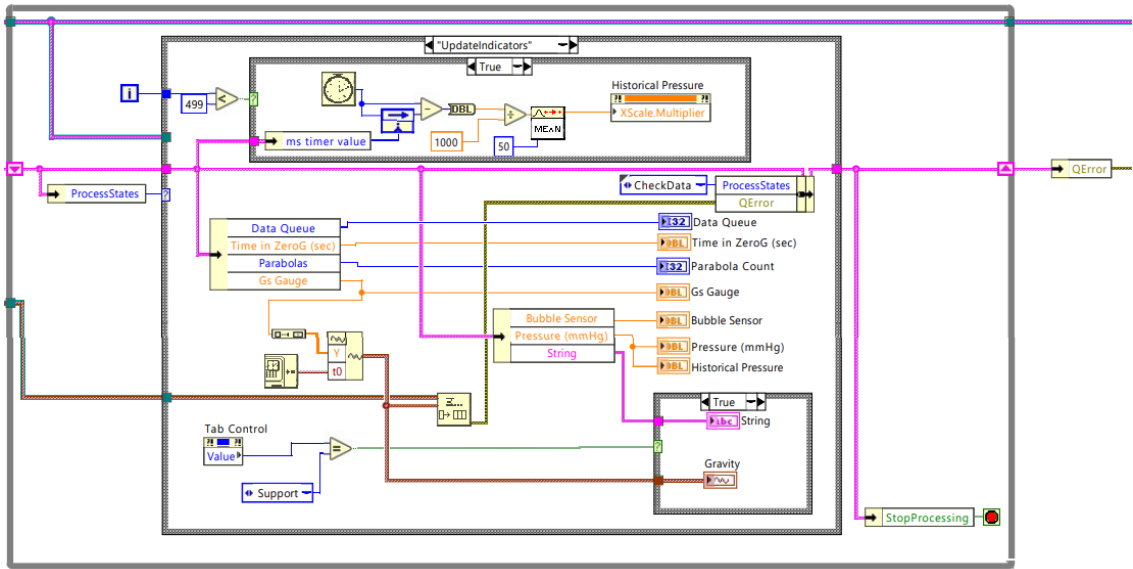


Figure 59: Close up of Visualization Loop

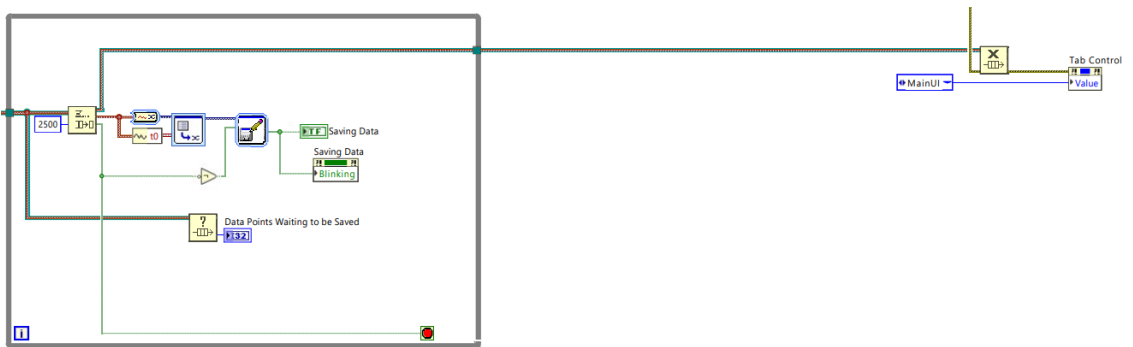


Figure 60: Close up of Data Saving Loop